

Novel light sources based on charged particles channeling in crystalline undulators

Andrey V. Solov'yov

MBN Research Center, Frankfurt am Main, Germany

www.mbnresearch.com

The ARIES workshop on Application of Crystals and Nanotubes for Beam Acceleration or Manipulation, ACN2020, Lausanne, Switzerland, March 10, 2020

- Introduction
 - » Oriented crystal based light sources
 - » Crystalline undulator based light sources
 - » Laser Compton scattering and CERN photon factory
 - » HORIZON2020 RISE-N-Light project
- Crystalline undulator
 - » Basic facts
 - » Feasibility of crystalline undulators
 - » Atomistic level computational modelling: MBN Explorer & MBN Studio
 - » Exemplar case studies
 - » Brilliance of crystalline undulators
- Conclusions and outlook

Selected examples of the novel Crystal based Light Sources (CLSs). Black circles and lines mark atoms of crystallographic planes, wavy curves show trajectories of the channeling particles, shadowed areas refer to radiation.

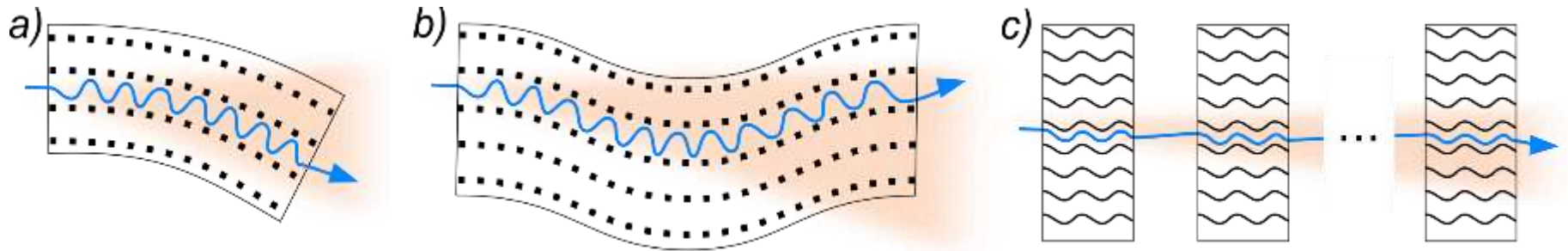


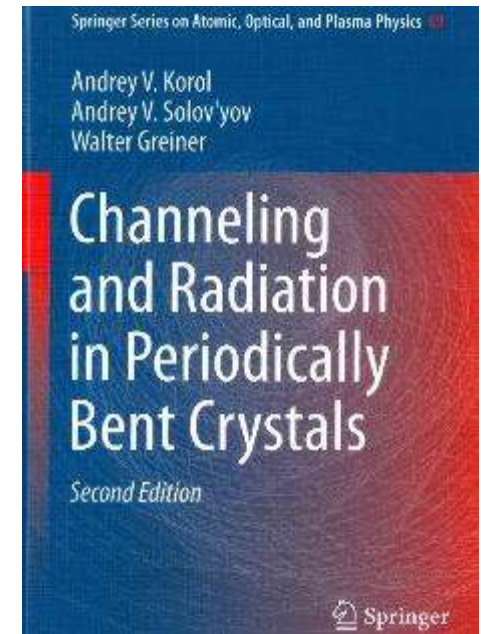
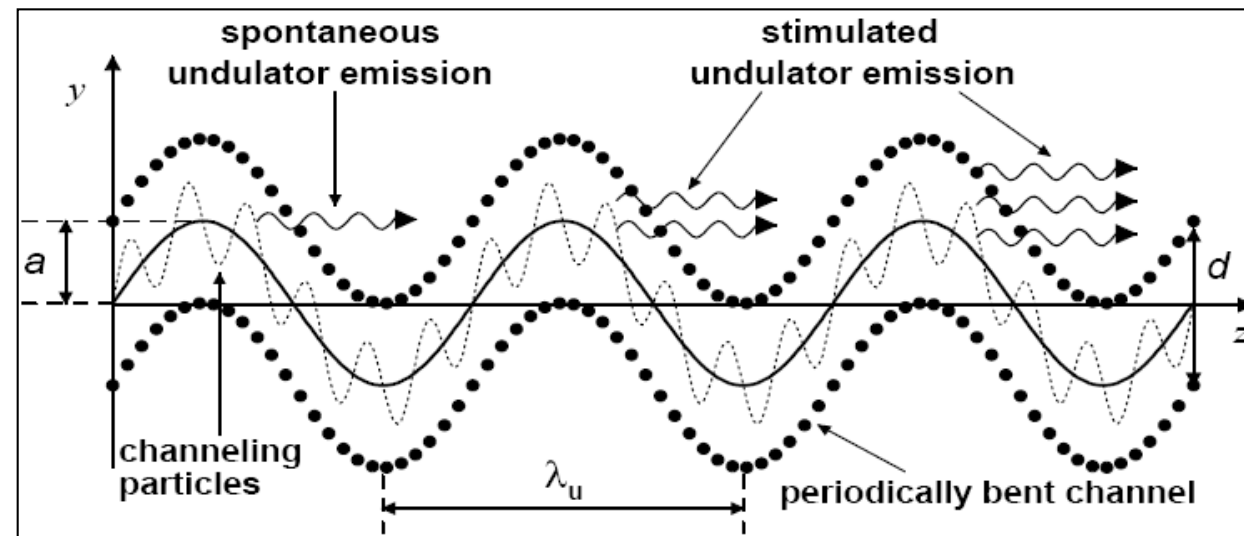
Figure from A.V. Korol, and A.V. Solov'yov, ArxiV 1910.13359 (2019)

A.V. Korol, A.V. Solov'yov, Greiner, *Channeling and Radiation in Periodically Bent Crystals*, Second Edition, Springer–Verlag, Berlin, Heidelberg (2014)

Radiation from a crystalline undulator

Basic idea (Korol, Solov'yov, Greiner, J.Phys.G, v.24, L45 (1998); **reviews:** *International Journal of Modern Physics E*, v.8, p.49-100 (1999); v.13, p.867-916 (2004)); PRL, 98, 164801, (2007); **Monograph**, Second Edition, Springer–Verlag, Berlin, Heidelberg (2014)

The radiation is generated by a bunch of ultra-relativistic positrons ($\varepsilon=0.5\ldots 10$ GeV) channeling in a crystal along periodically bent crystallographic planes. The periodicity of trajectories results in the undulator-type radiation due to the constructive interference of the photons emitted from similar parts of the trajectory.



$d=1\ldots 2 \text{ \AA}$ - the interplanar spacing
 $a=(10\ldots 50)d$ - the amplitude of bending
 $\lambda_u=(10^4\ldots 10^5)a$ - the period of bending

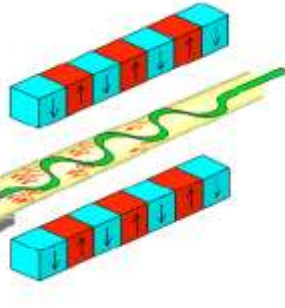


$$d \ll a \ll \lambda$$

Crystalline vs magnetic undulator

Magnetic undulator:

$$\lambda_u \sim 1 \text{ cm}, \hbar\omega \sim 10 \text{ keV}$$



Crystalline undulator:

$$\lambda_u \sim 10 \mu\text{m}, \hbar\omega \sim 0.1 \dots 10 \text{ MeV}$$

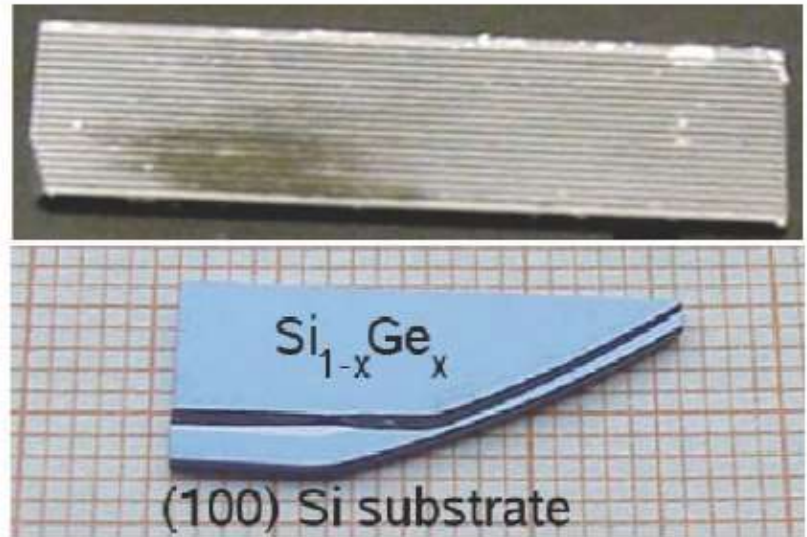


Fig. 1.3 *Left:* Magnetic undulator for the X-ray laser XFEL [179]. The picture is taken from [180]. *Right top:* laser-ablated diamond crystal. The crystal size is $4 \times 2 \times 0.3 \text{ mm}^3$. The undulator period is $\lambda_u = 50 \mu\text{m}$. The picture is taken from [74]. *Right bottom:* a $\text{Si}_{1-x}\text{Ge}_x$ superlattice crystalline undulator with four periods. Periodically varied Ge content (from $x = 0$ to $x_{\text{max}} = 0.5\%$) gives rise to the undulator period $\lambda_u = 50 \mu\text{m}$. The picture is courtesy of J.L. Hansen, A. Nylandsted and U. Uggerhøj (University of Aarhus).

CU-LS versus LS based on scattering of laser photons

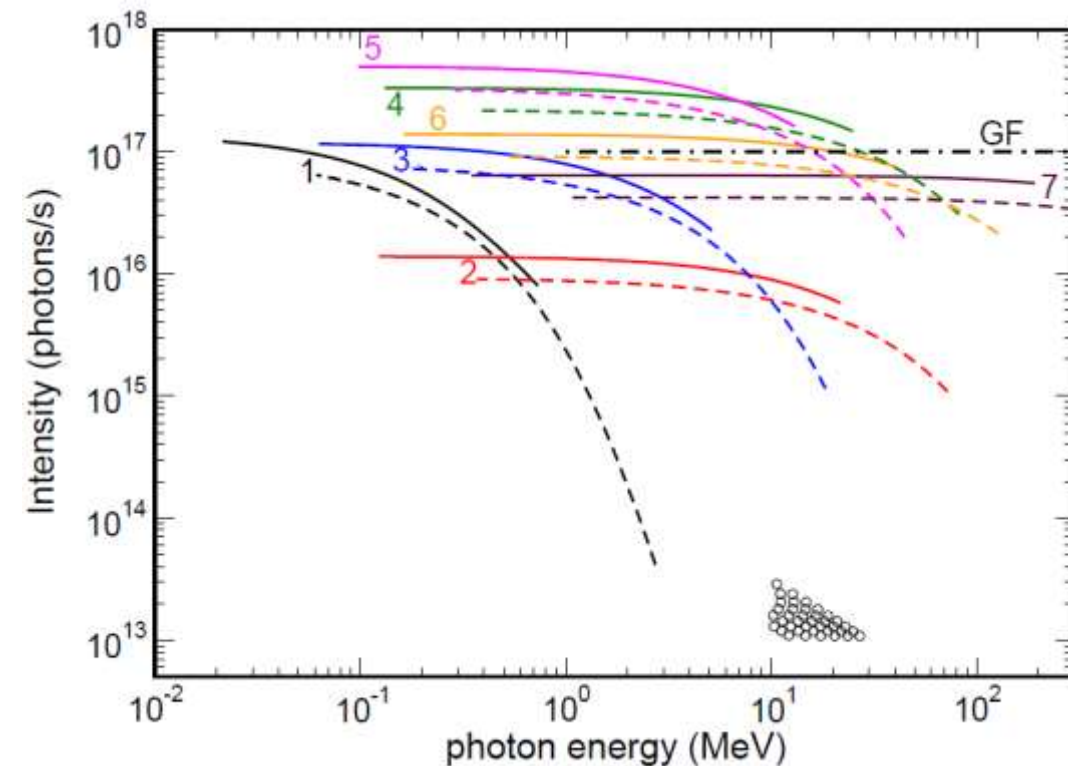
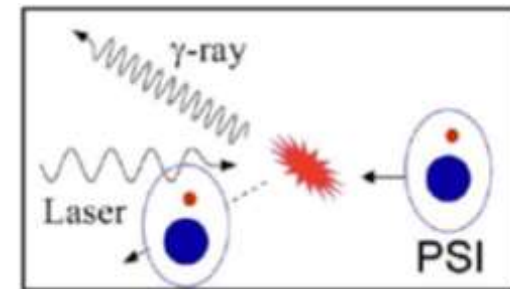


Figure 4. Peak intensity (number of photons per second, $\Delta N_{\omega} I_{\max}/e$) of diamond(110)-based CUs calculated for positron beams at different facilities: 1 - DAΦNE, 2 - VEPP4M, 3 - BEPC-II, 4 - SuperB, 5 - SuperKEK, 6 - FACET-II, 7 - CEPC. Solid and dashed lines correspond to the emission in the first and third harmonics, respectively. Open circles indicate the data on the laser-Compton backscattering [42]. The horizontal dash-dotted line marks the intensity 10^{17} photon/s indicated in the Gamma Factory (GF) proposal for CERN [3].

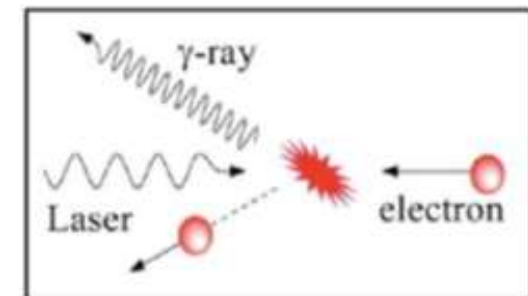
A.V. Korol, A.V. Solov'yov, Arxiv 1910.13359 (2019)

GF: Gamma Factory proposal for CERN by W. Krasny *et al*

Resonant absorption of laser photons by Partially Stripped Ions (PSIs)



Compton scattering of laser photons by Partially Stripped Ions (PSIs)



Brilliance of a photon source relates the number of photons of a given energy emitted per unit time interval, unit source area, unit solid angle and per bandwidth:

$$B_n = \frac{\Delta N_{\omega_n}}{10^3 (\Delta \omega_n / \omega_n) (2\pi)^2 \varepsilon_x \varepsilon_y} \frac{I}{e}$$

n – harmonic number

$\omega_n, \Delta \omega_n$ – energy and width of the n th harmonic

$\Delta \omega_n / \omega_n$ – bandwidth (=BW)

ΔN_{ω_n} – number of photons with
 $\omega \in [\omega_n - \Delta \omega_n / 2, \omega_n + \Delta \omega_n / 2]$

I – electric current of the beam

$\varepsilon_{x,y}$ – emittance of the photon source along

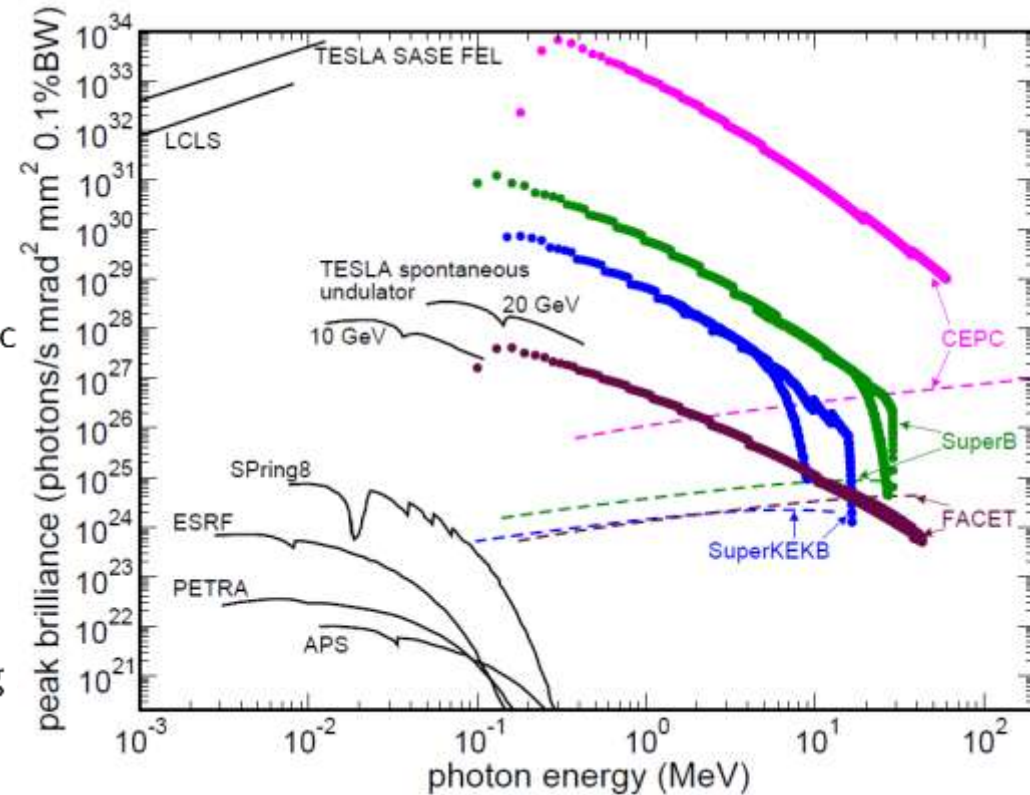


Figure 5. Peak brilliance of superradiant CUR (thick solid curves) and spontaneous CUR (dashed lines) from diamond(110) CUs calculated for the SuperKEKB, SuperB, FACET-II and CEPC positron beams versus modern synchrotrons, undulators and XFELs.

A.V Korol, A.V Solov'yov, Arxiv 1910.13359 (2019)

Horizon 2020 project N-LIGHT : Novel Light Sources: Theory and Experiment MSCA Research and Innovation Staff Exchange (RISE)



JOHANNES GUTENBERG
UNIVERSITÄT MAINZ



University of
Kent



**Peter the Great St. Petersburg
Polytechnic University**



**H2020 N-LIGHT continues research conducted
within FP6-PECU, FP7-CUTE, H2020-PEARL**



Crystalline undulator

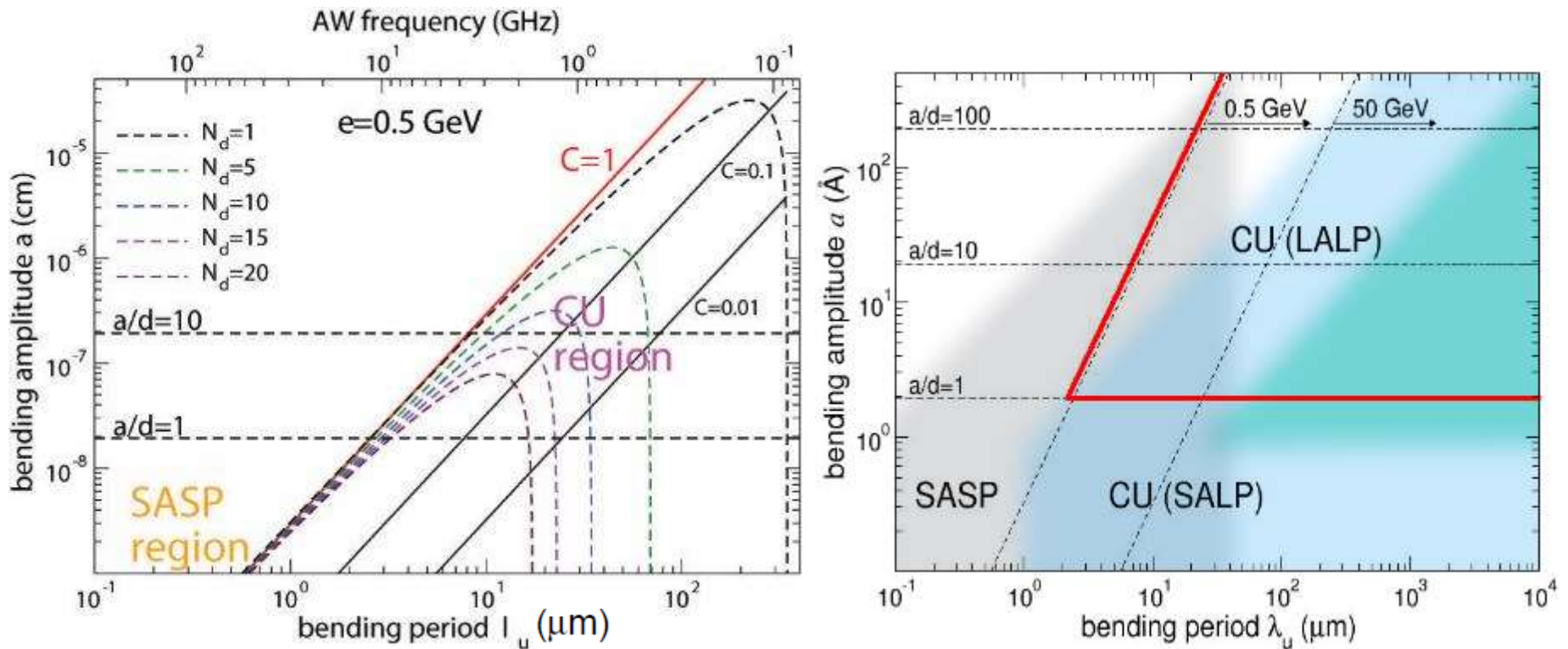
The summary of all essential conditions (Korol, Solov'yov, Greiner 1998, 2004):

$$\left\{ \begin{array}{ll} C = (2\pi)^2 \frac{\varepsilon}{qU'_{\max}} \frac{a}{\lambda^2} \ll 1 & \text{stable channeling} \\ d \ll a \ll \lambda & \text{large-amplitude regime} \\ N = \frac{L}{\lambda} \gg 1 & \text{large number of undulator periods} \\ L \leq \min [L_d(C), L_a(\omega)] & \text{account for the dechanneling} \\ & \text{and photon attenuation} \\ \frac{\Delta\varepsilon}{\varepsilon} \ll 1 & \text{low radiative losses} \end{array} \right.$$

If these are met then:

- within the length L the particle experiences stable planar channeling
- characteristic energies of the undulator and channeling radiation are well separated
- intensity of the undulator radiation is higher than that of the channeling radiation.
- emission spectrum is stable towards the radiative losses.

CU parameter ranges



Left figure. Bending amplitude, a , vs bending period, λ , consistent with the condition $C < 1$ and calculated for various numbers of undulator periods N_d as indicated for $e=0.5$ GeV ($\gamma = 10^3$) positron channeling in Si along (110) crystallographic plane. Bending profile $y = a \sin(2\pi z/\lambda)$.

A.Korol, W.Krause, A.Solov'yov, W.Greiner, J.Phys.G: Nucl.Part.Phys., v.26, L87-L95 (2000);

From A.Korol, A.Solov'yov, W.Greiner, Chan. and Rad. In Periodically Bent Crystals, Second Edition, Springer-Verlag, Berlin, Heidelberg (2014);

Right figure. Shadowing indicates the ranges accessible by means of modern technologies: superlattices (grey), surface deformations (green), AWs (blue); **From Korol, Solov'yov, Arxiv 1910.13359 (2019)**



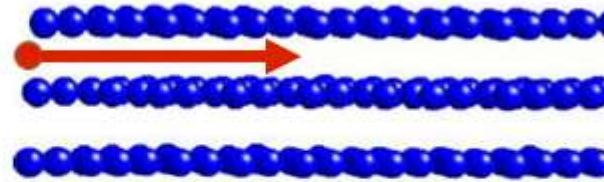
Channeling and channeling radiation: basic facts

Channeling process

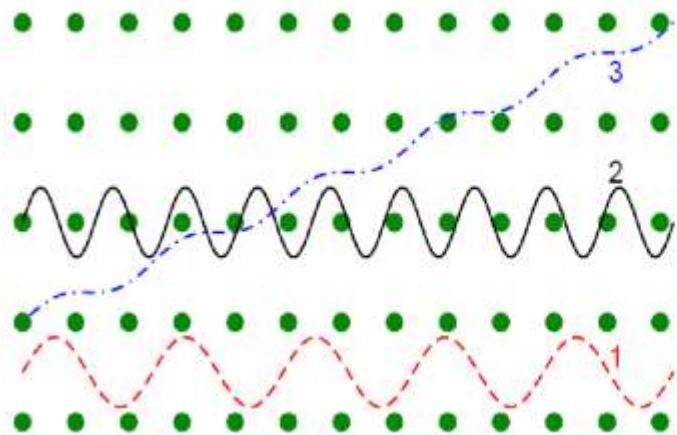
Channeling is the process of propagation of charged relativistic particle through the crystal along one of it's planes or axes.



Silicon crystal seen along the $\langle 100 \rangle$ axis.



Si (110) planar channels seen from a random direction.



over-barrier particle

channeling electron

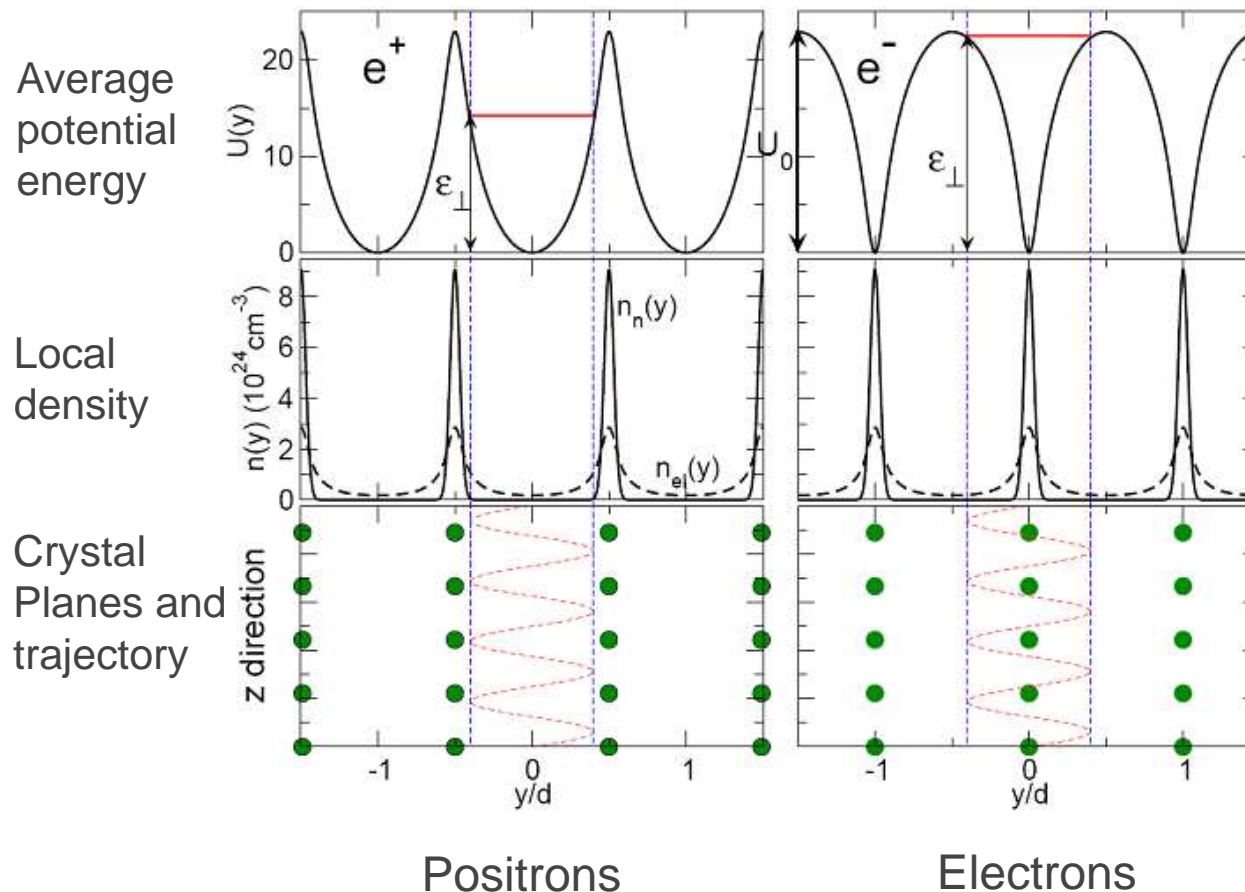
channeling positron

Crystal planes and axis guide movement of electrons and positrons through the crystal.

Positrons repel from crystal planes.
Electrons attract to planes.

Both types of particles can move along planes with periodic oscillation (channeling motion), leave (dechanneling) or return to the channel (rechanneling).

Figures from Korol, Solov'yov, Greiner, J.Phys.G, v.24, L45 (1998);
International Journal of Modern Physics E, v.8, p.49-100 (1999)

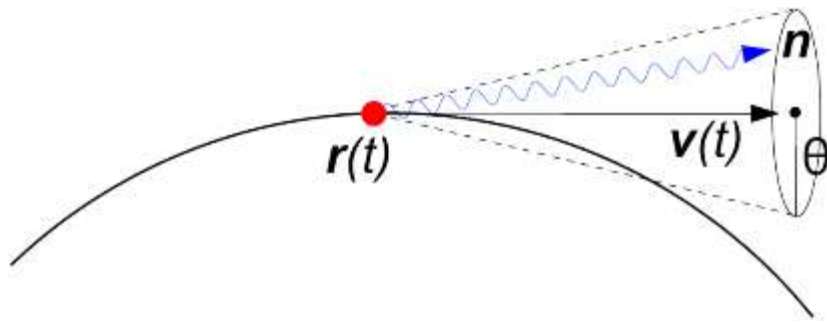


The channeling process can be treated in terms of average potential of interaction between projectile and crystalline planes.

Electron and positrons have different average potential. This leads to different characteristics of trajectories for electron and positron.

Figures from Korol, Solov'yov, Greiner (1997, 1998)

Spectral and angular distribution of photons



Accelerated motion of charged projectiles produces radiation.

The radiation is mostly emitted in a small cone around instant velocity.

For each trajectory the radiation spectrum was calculated using the quasi-classical method* taking into account the recoil due to the photon emission.

$$\frac{dE(\theta < \theta_{max})}{\hbar d\omega} = \int_0^{2\pi} d\phi \int_0^{\theta_{max}} \theta d\theta \frac{d^3 E}{\hbar d\omega d\Omega}$$

$$\frac{d^3 E}{\hbar d\omega d\Omega} = \frac{\alpha q^2 \omega^2}{4\pi^2} \frac{1}{2} \int_{-\infty}^{\infty} dt_1 \int_{-\infty}^{\infty} dt_2 e^{i\omega'(\psi(t_1) - \psi(t_2))} \left[(1 + (1 + u)^2) (\vec{\beta}(t_1) \cdot \vec{\beta}(t_2) - 1) + \frac{u^2}{\gamma^2} \right]$$

$$\vec{\beta}(t) = \vec{v}(t)/c \quad \psi(t) = t - \vec{n} \cdot \vec{r}(t)/c$$

$$u = \hbar\omega/(\varepsilon - \hbar\omega) \quad \omega' = \omega(1 + u)$$

* V.N. Baier, V.M. Katkov, V.M. Strakhovenko, Electromagnetic Processes at High Energies in Oriented Single Crystals. World Scientific, Singapore (1998).

Spectral and angular distribution of spontaneous radiation in CU

$$\frac{dE_N}{d\omega d\Omega_{\mathbf{n}}} = D_N(\eta) F(\omega; \gamma, p; \theta, \varphi)$$

Here, $F(\omega; \gamma, p; \theta, \varphi)$ is a smooth function of the arguments

$$D_N(\eta) = \left(\frac{\sin N\pi\eta}{\sin \pi\eta} \right)^2$$

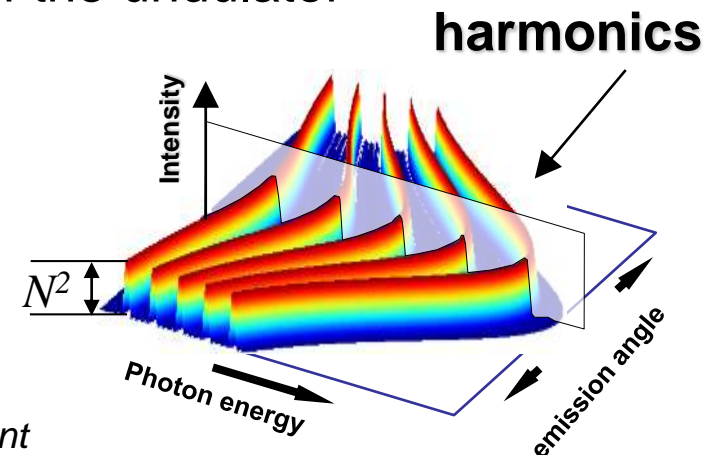
$$\omega^{(K)} = \frac{4\gamma^2 \Omega_u K}{2 + 2\theta^2 \gamma^2 + p^2}, \quad K = 1, 2, \dots$$

$$\eta = \frac{\omega}{\Omega_u} \left(\frac{1}{2\gamma^2} + \frac{\vartheta^2}{2} + \frac{p^2}{4\gamma^2} \right)$$

The characteristic frequencies (harmonics) of the undulator radiation

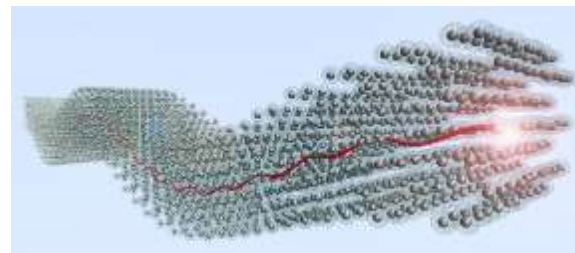
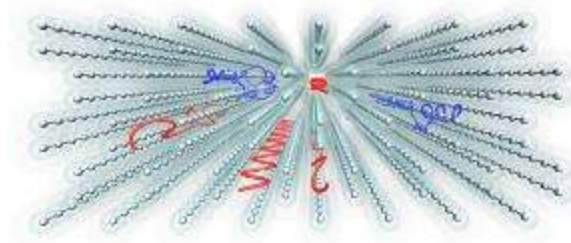
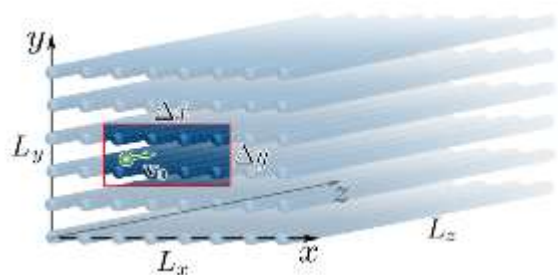
$$p^2 = 2\gamma^2 \frac{\dot{y}^2}{c^2}$$

p is undulator parameter
dipole regime: $p \ll 1$
non-dipole regime: $p \gg 1$

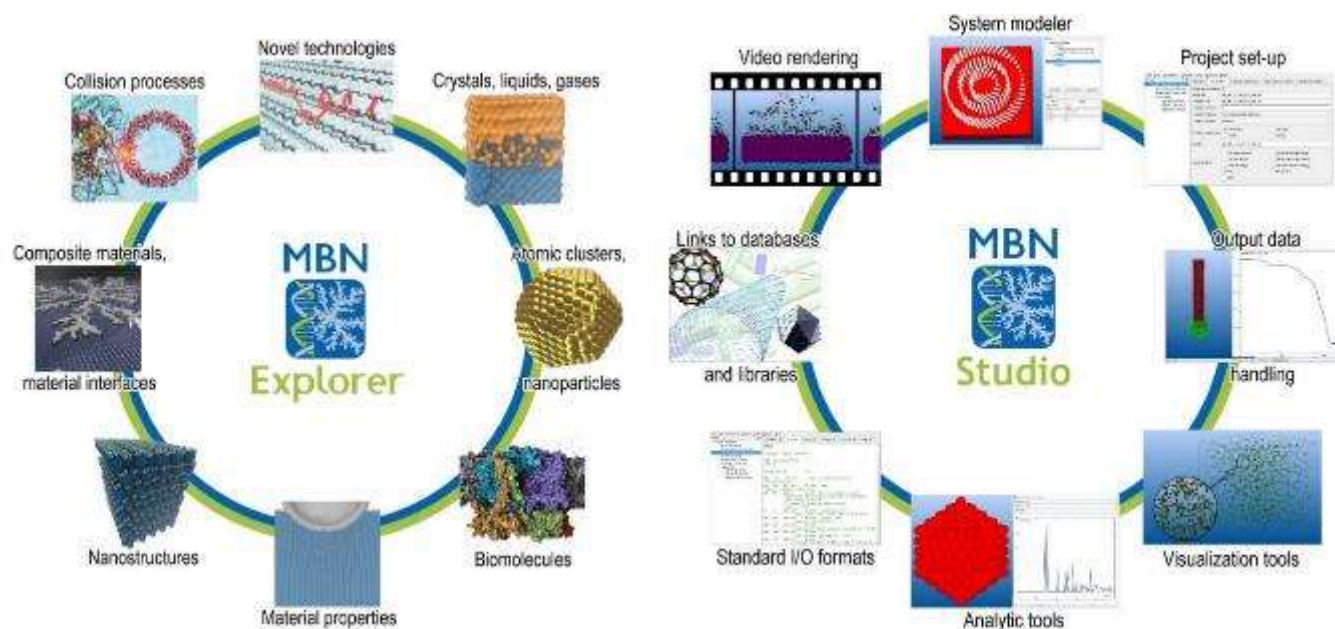


A.Korol, A.Solov'yov, W.Greiner, *Chan. and Rad. In Periodically Bent Crystals*, Second Edition, Springer-Verlag, Berlin, Heidelberg (2014)

Atomistic simulations of ultrarelativistic charged particle propagation and radiation in media by means of MBN Explorer and MBN Studio software packages



MBN Explorer & MBN Studio software: a 'computational microscope'



MBN Explorer and MBN Studio are being developed by the MBN Research Center www.mbnresearch.com in Frankfurt.
I.A. Solov'yov, A.V. Yakubovich, P.V. Nikolaev, I.Volkovets, and A.V. Solov'yov, *Meso Bio Nano Explorer -- a universal program for multiscale computer simulations of complex molecular structure and dynamics*, Journal of Computational Chemistry, volume 33, pp. 2412-2439 (2012).
I.A. Solov'yov, A.V. Korol, A.V. Solov'yov, *Multiscale modelling of complex molecular structure and dynamics with MBN Explorer*, Monograph, Springer International Publishing, Cham, Switzerland 480 pp. (2017)

MBN Explorer

Energy calculation

Dynamic tasks

System optimisation

Kinetic Monte Carlo algorithms

Molecular dynamics : nonrelativistic, Euler, reactive MD, IDMD, relativistic

Model parameters

Particles' displacements, diffusion, coalescence and dissociation probabilities, spatial grids, stochastic evolution time steps, particle creation, annihilation, reactions, duration of processes

Pairwise potentials

Lennard-Jones, Exponential, Power, Coulomb, Dzugutov, Girifalco, Morse, Molière, Yukawa, Pacios, Quasi Sutton-Chen, Ziegler-Biersack-Littmark

Many body potentials

Sutton-Chen, Gupta Brenner Tersoff Finnis-Sinclair Stillinger-Weber Tabulated EAM

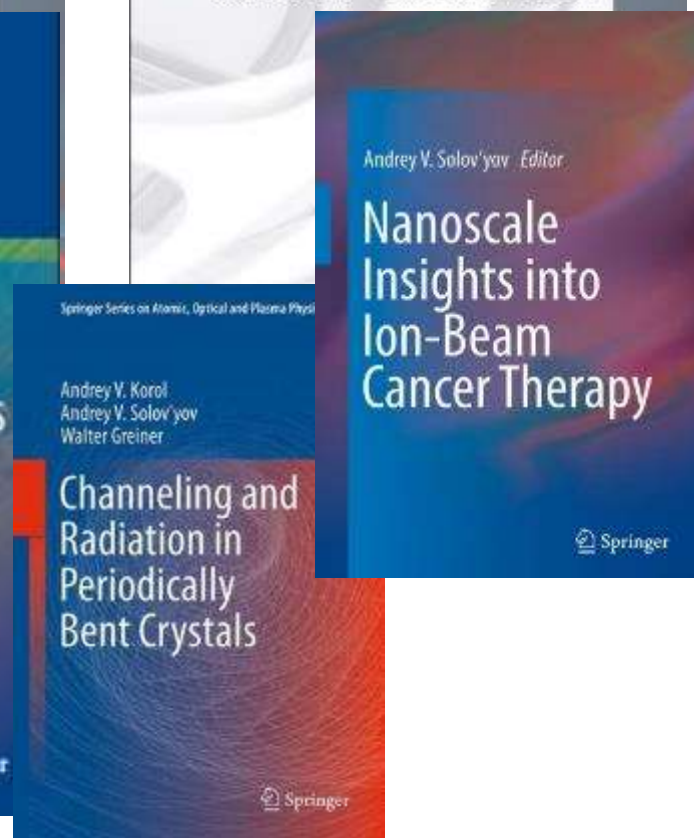
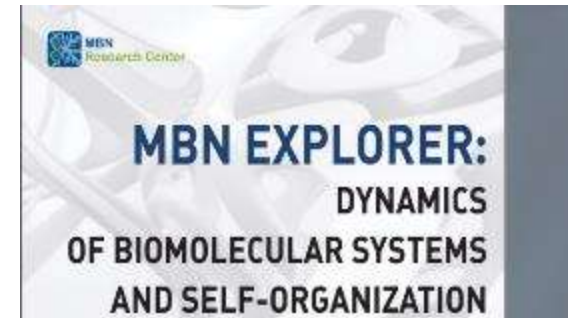
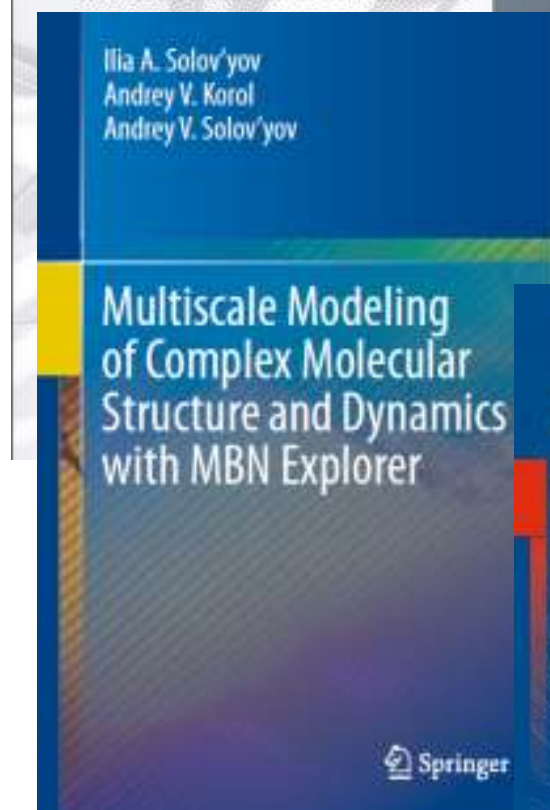
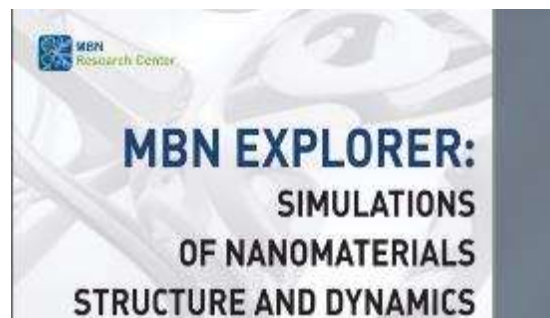
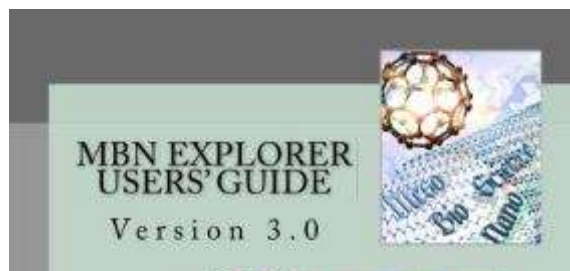
Force fields

CHARMM
Reactive CHARMM
Reactive FFs

External fields

Electric
Viscous
Gravitational

MBN Explorer and MBN Studio books

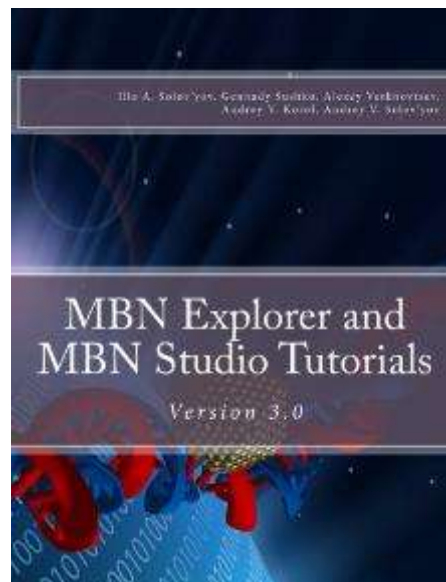


MBN Explorer & MBN Studio Tutorials and Conferences



MBN Research Center organises regular hands-on tutorials on MBN Explorer & Studio aimed at the presentation of the implemented physical models and computational approaches.

The training course is based on practical exercises on setting up simulations of MBN systems structure and dynamics, visualisation and analysis of simulated data.



www.isacc-portal.org

The Ninth International Symposium
"Atomic Cluster Collisions"



School of Physical Sciences, University of Kent
Canterbury, United Kingdom
July 31 – August 03, 2019



FIRST ANNOUNCEMENT

**CECAM-HQ-EPFL
Lausanne
Switzerland
June 3-5, 2020**
[https://www.cecarn.org/
workshops2020/](https://www.cecarn.org/workshops2020/)



**DySoN 2020,
November 23-27,
Santa Margherita
Ligure, Italy**

International Conference
"Dynamics of Systems on the Nanoscale"
DySoN Conference 2018
Steigenberger Hotel Sanssouci, Potsdam, Germany
October 08 – 12, 2018



FIRST ANNOUNCEMENT

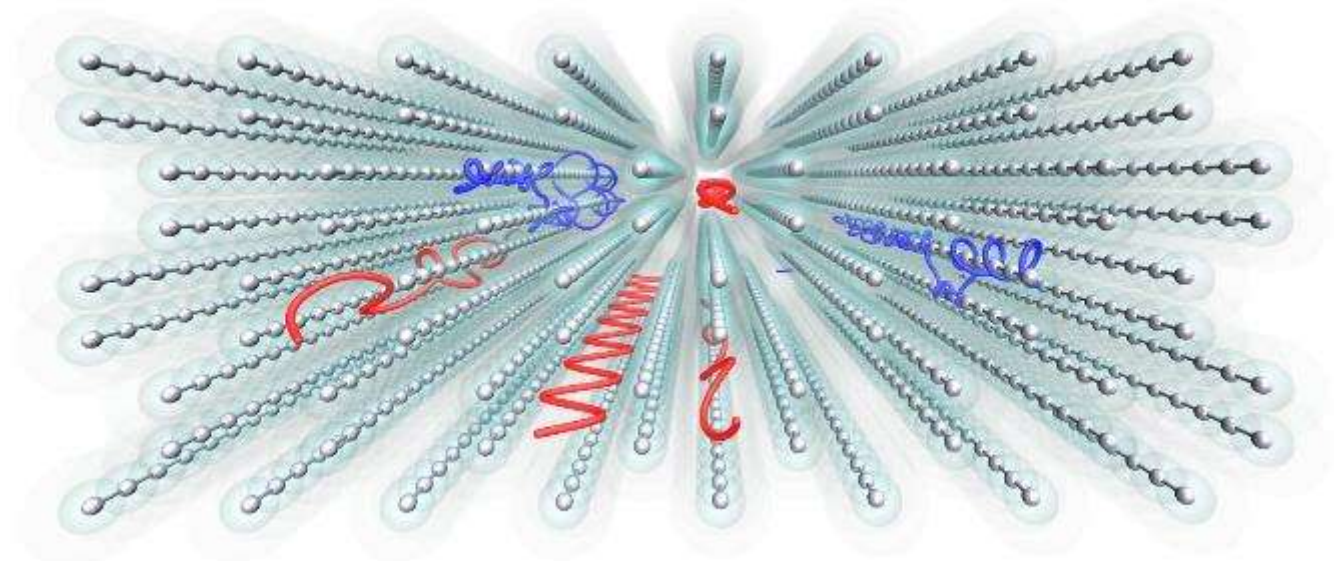
www.dyson-conference.org

Simulation of motion of relativistic particles in MBN Explorer is based on relativistic equations of motion.

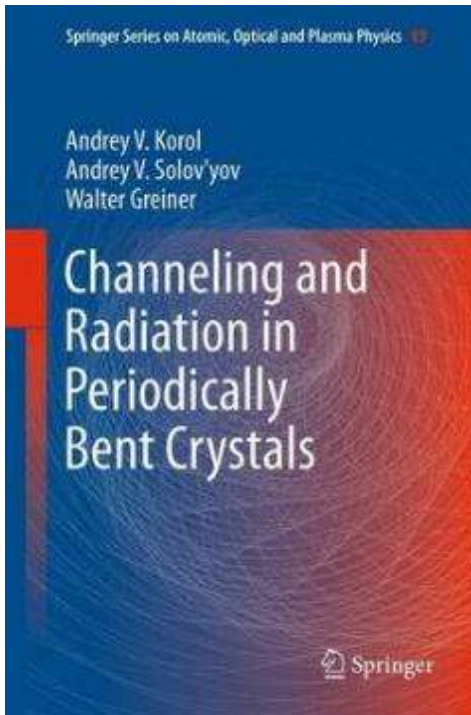
$$\begin{cases} \dot{\mathbf{v}} = \frac{1}{m\gamma} \left(\mathbf{F} - \mathbf{v} \frac{(\mathbf{F} \cdot \mathbf{v})}{c^2} \right) \\ \dot{\mathbf{r}} = \mathbf{v} \end{cases}$$

This system of equations is strongly nonlinear and requires the use of high-order integrator in order to be solved correctly.

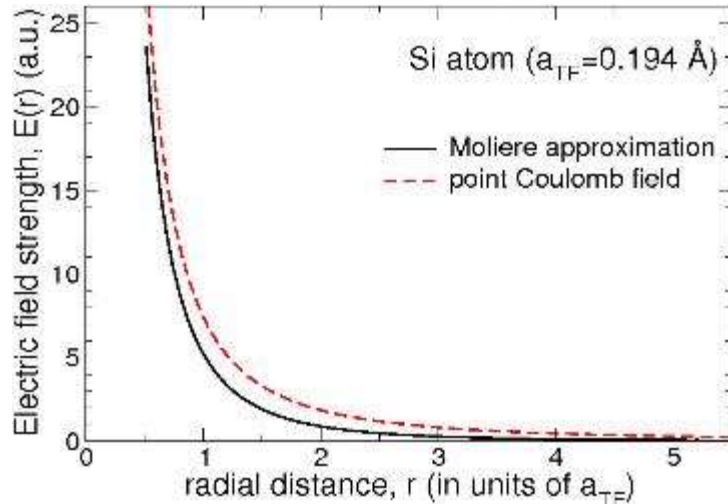
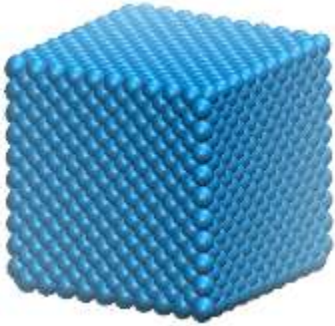
$$\gamma = \frac{1}{\sqrt{1 - v^2/c^2}}.$$



The developed approach (G.B. Sushko, V.G. Bezchastnov, I.A. Solov'yov, A.V. Korol, W. Greiner, A.V. Solov'yov, Journal of Computational Physics, 252, 404 (2013)) is not restricted to the crystalline medium and is applicable to describe the propagation of ultra-relativistic projectile in an arbitrary medium.



➤ Crystalline structure



- Each atom – a source of static potential treated in the **Moliele approximation**:

$$U_{\text{at}}(r) = \frac{Ze}{r} \chi(r)$$

$$\chi(r) = \sum_{i=1}^3 \alpha_i \exp\left(-\frac{\beta_i r}{a_{\text{TF}}}\right)$$

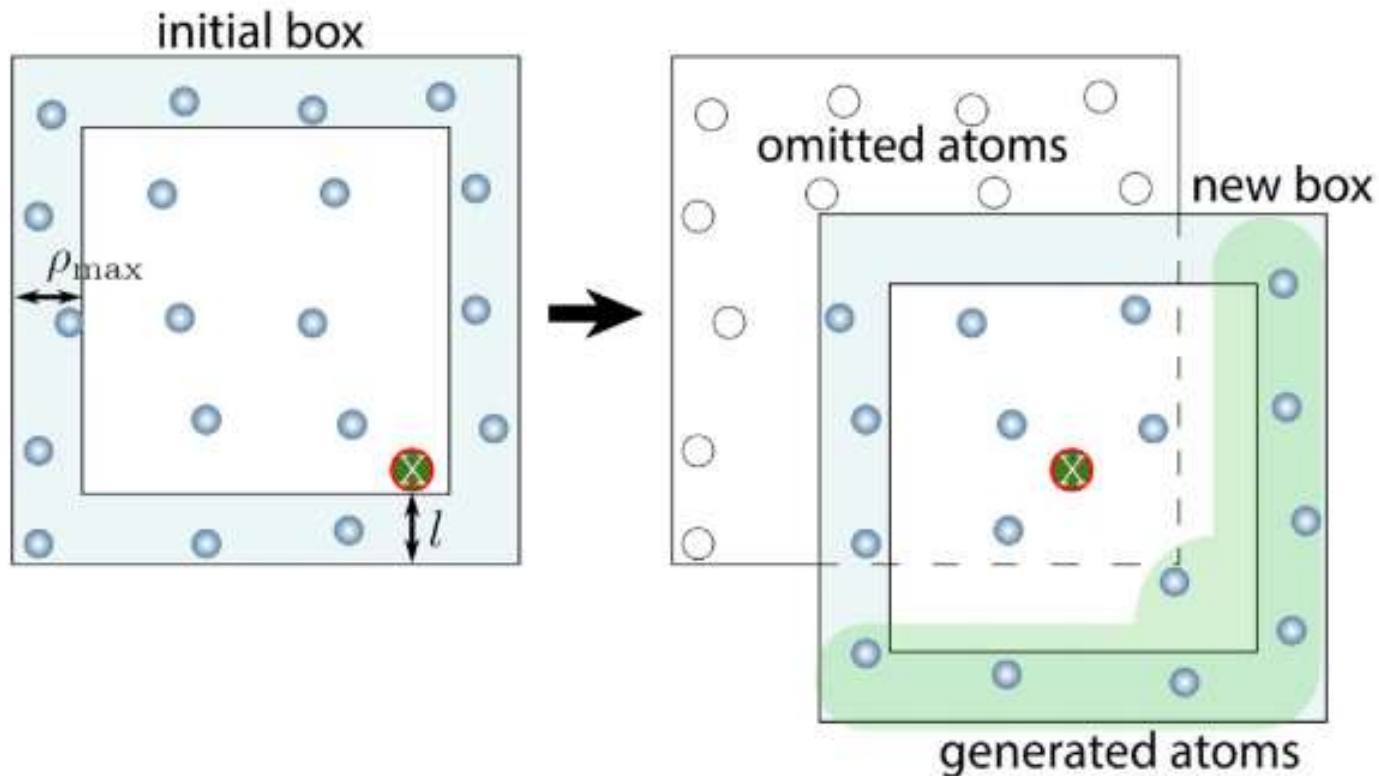
$$\begin{cases} \alpha_1 = 0.35, \alpha_2 = 0.55, \alpha_3 = 0.1 \\ \beta_1 = 0.3, \beta_2 = 1.2, \beta_3 = 6.0 \end{cases}$$

$$a_{\text{TF}} = \frac{0.8853}{Z^{1/3}} a_{\text{B}}$$

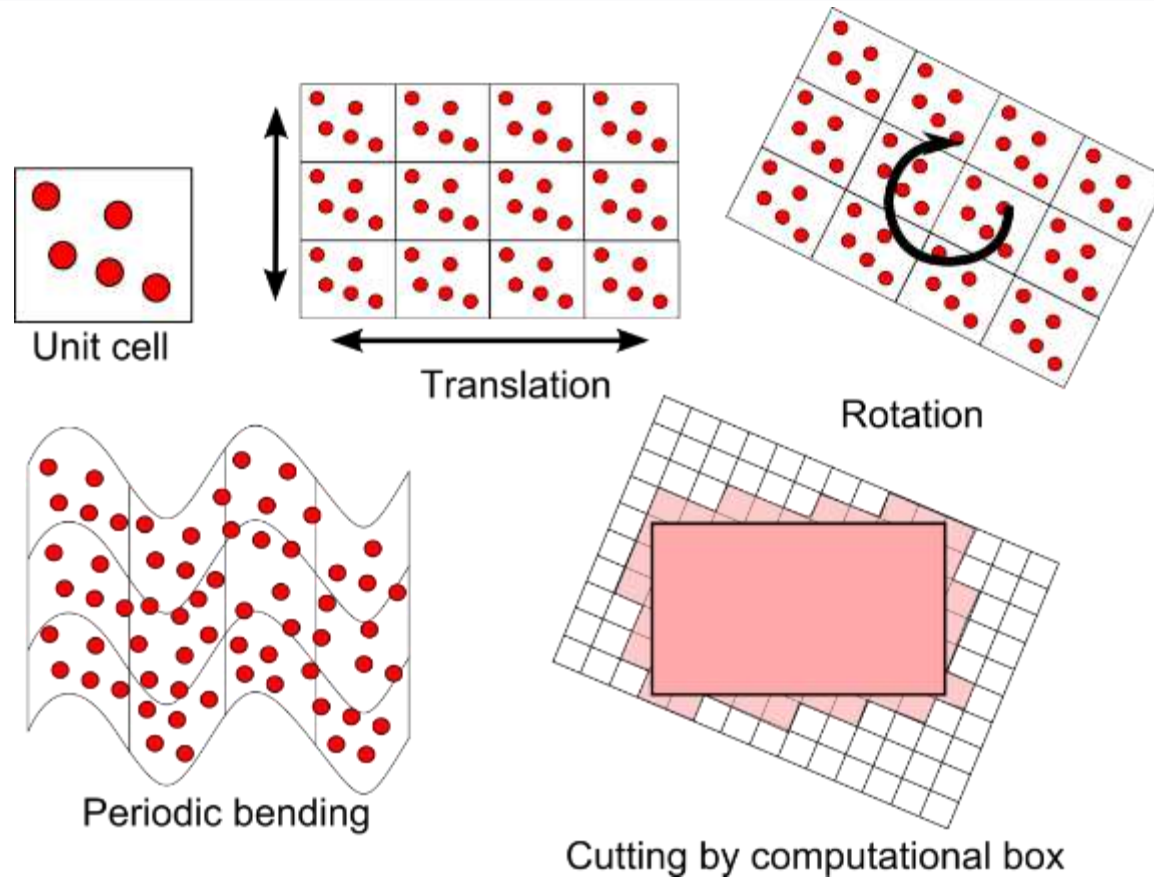
$$\mathbf{E}_{\text{at}}(\mathbf{r}) = -\frac{\partial U_{\text{at}}}{\partial \mathbf{r}} = Ze \frac{\mathbf{r}}{r^3} [\chi(r) - r\chi'(r)]$$

- **Pacios potential**
- **Binary crystalline structures**

MBN Explorer algorithm for accounting for interatomic interactions



The motion of a projectile is simulated through the generated crystalline structure in which atoms are fixed in space and act only as a source of an external field for the projectile. The simulation box is reduced to a close vicinity of a projectile in which the actual interaction takes place. This simulation box follows the projectile. The atoms of the crystal are generated dynamically in this box and are omitted after the particle passage.



Description of a crystalline medium is fulfilled through a setting of a crystalline unit cell and a set of its transformations. These transformations allow efficient generation of the desired crystalline structure at any domain in the space.

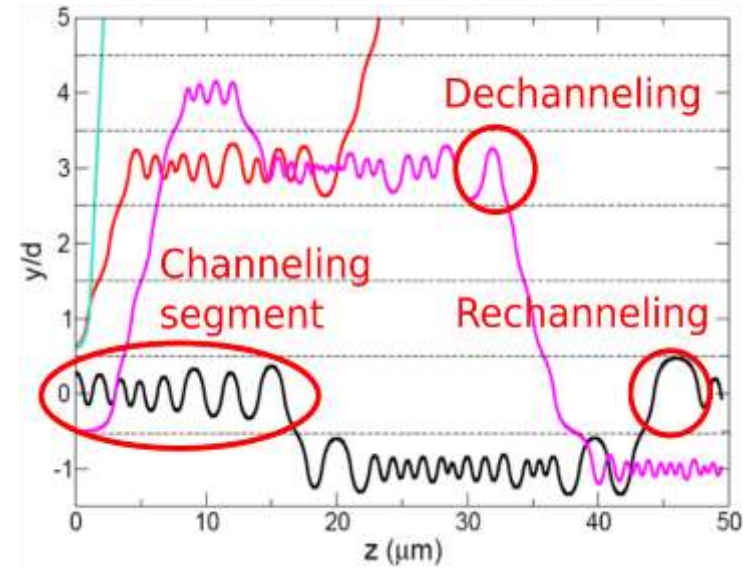
Simulated trajectories are analyzed further to calculate/estimate:

➤ Acceptance:

$$\mathcal{A} = \frac{N_{\text{acc}}}{N_0}$$

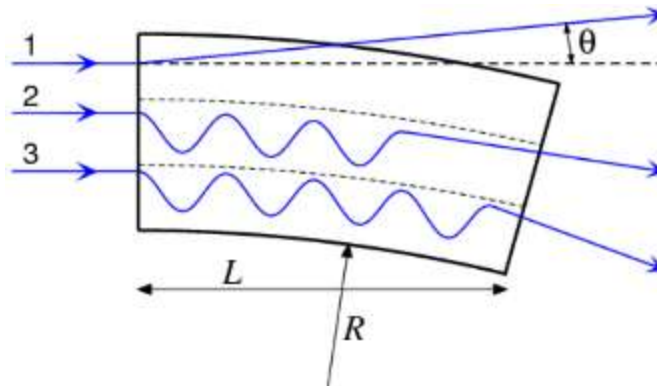
➤ Fractions of channeling particles:

$$\begin{cases} \xi_{\text{ch0}}(z) = \frac{N_{\text{ch0}}(z)}{N_0} \\ \xi_{\text{ch}}(z) = \frac{N_{\text{ch}}(z)}{N_0} \end{cases}$$



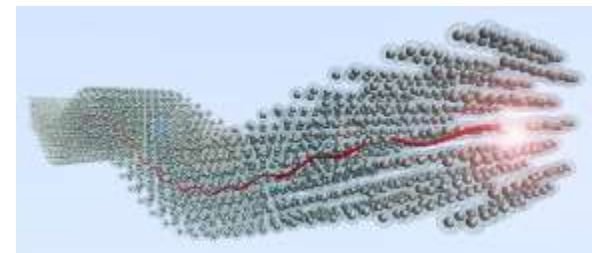
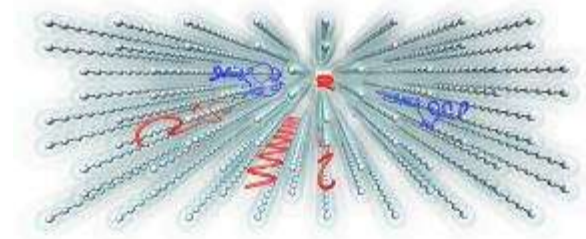
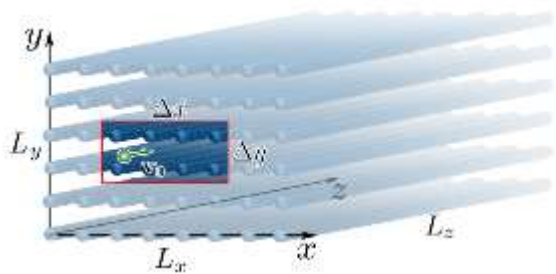
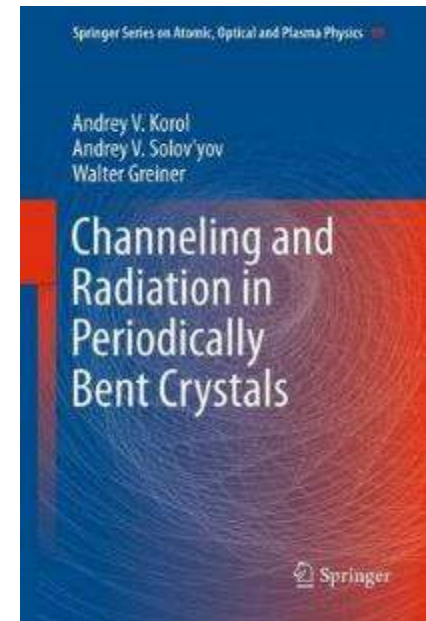
➤ Dechanneling length: $N_{\text{ch}}(z) \propto N_0 \exp(-z/L_d)$

➤ Distribution in the deflection angle



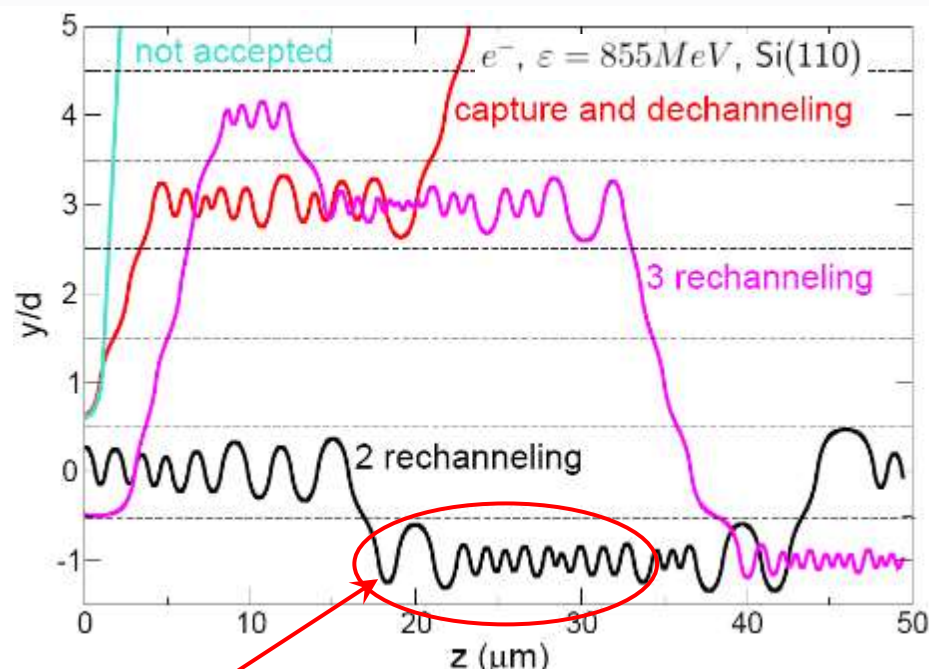


Exemplar case studies

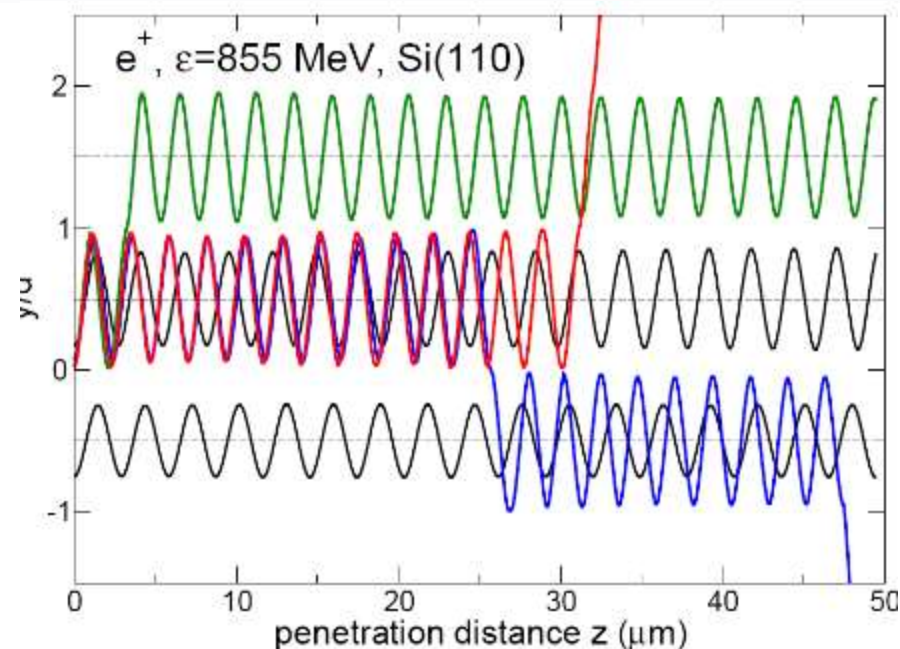
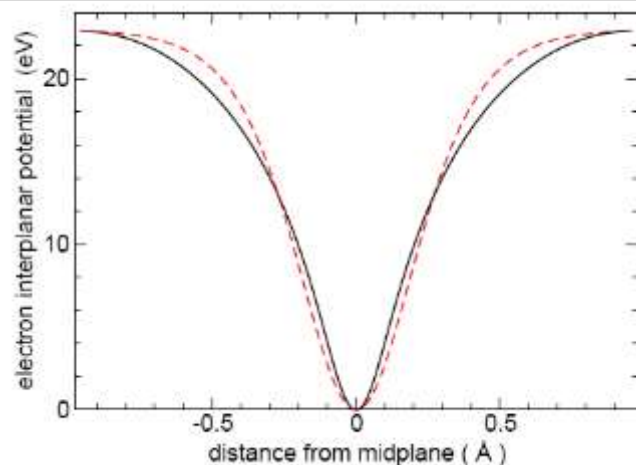


- **6.7 GeV e^\pm in straight Si(110)** (Sushko, Bezchastnov, I. A. Solov'yov, Korol, Greiner, A.V. Solov'yov, J. Comp. Phys. 252, 404 (2013))
- **270 – 855 MeV e^\pm in straight, bent and periodically bent Si(110) & Si(111)** (Sushko, Korol, Solov'yov, et al. J. Phys. Conf. Ser. **438** (2013) 012018; **438** (2013) 012019; Eur. Phys. J. D **68**, 268 (2014))
- **Channeling of ultra-relativistic positrons in bent diamond crystals** (Sushko, Korol, Solov'yov, et al. SPbTU J. Phys. Math. **1** (2015) 212-218).
- **A small-amplitude crystalline undulator based on 20 GeV electrons and positrons.** (Sushko, Korol, Solov'yov. *SPbTU J. Phys. Math.* **1** (2015) 341-345))
- **Simulation of channeling and radiation of 855 MeV e^\pm in a small-amplitude short-period crystal** (Bezchastnov, Korol, Solov'yov, *NIMB* **387** (2016) 41-53).
- **Multi-GeV e^\pm channeling in bent Si (111)** (Sushko, Korol, Solov'yov. *NIMB* **355** (2015) 39-43).
- **Radiation from multi-GeV e^\pm in periodically bent Si crystal.** (Bezchastnov, Korol, Solov'yov. *J. Phys. B* **47** (2014) 195401)
- **855 MeV e^\pm in SASP Si(110)** (H. Shen Q. Zhao, F.S. Zhang, Sushko, Korol, Solov'yov, *NIMB* **424** (2018) 26-36).
- **Channeling and radiation by 855 MeV electrons enhanced by re-channeling in periodical-ly bent diamond crystal.** (Bezchastnov, Korol, Solov'yov. *Eur. Phys. J. D* **71** (2017) 174)
- **Channeling and Radiation of 855 MeV Electrons and Positrons in Straight and Bent Tungsten (110) Crystals.** (H. Shen, Q. Zhao, F.S. Zhang, G.B. Sushko, A.V. Korol, A.V. Solov'yov, *Nuclear Instruments and Methods in Physics Research B*, **424**, 26–36 (2018))
- **Interplay and specific features of radiation mechanisms of electrons and positrons in crystalline undulators.** (A.V. Pavlov, A.V. Korol, V.K. Ivanov, A.V. Solov'yov, *J. Phys. B: At. Mol. Opt. Phys.*, **52**, 11LT01 (2019))
- **Radiation of 375 MeV electrons and positrons curing channeling in straight and periodically bent diamond crystals,** (A.V. Pavlov, A.V. Korol, V.K. Ivanov, A.V. Solov'yov, *St. Petersburg State Polytechnical University Journal. Physics and Mathematics*, **12**(4), 108-118 (2019))
- **Channeling of electrons and positrons in straight and periodically bent diamond(110) crystals,** A.V. Pavlov, A.V. Korol, V.K. Ivanov, A.V. Solov'yov, *Eur. Phys. J. D*, **74**, 21 (2020))

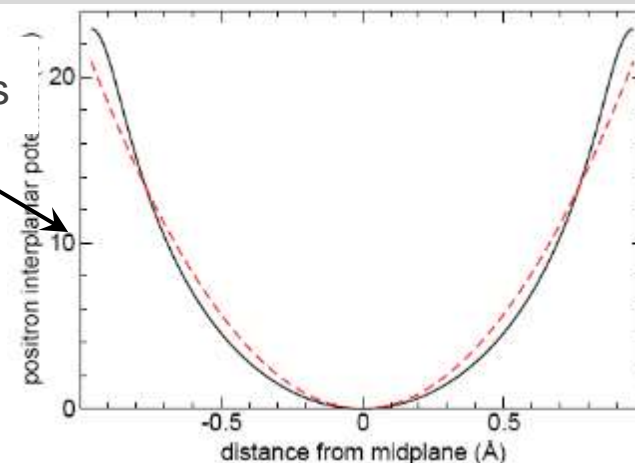
Electron vs positron simulations



Strong anharmonicity: $T_{\text{ch}} = T_{\text{ch}}(a_{\text{ch}})$

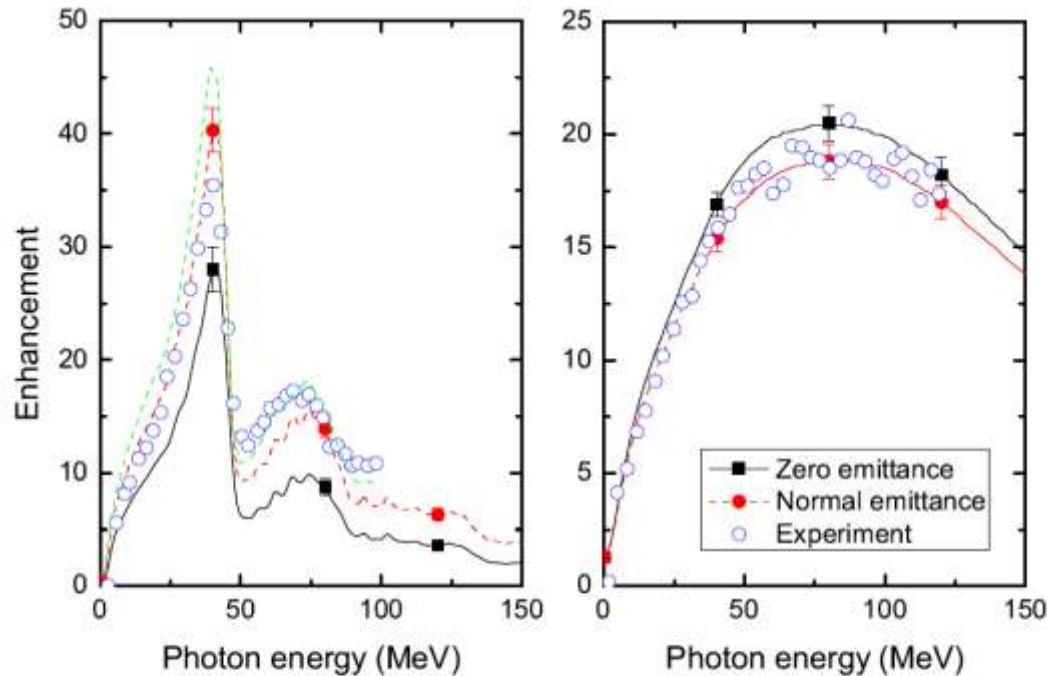


Nearly harmonic: $T_{\text{ch}} \approx \text{const}$



interplanar potentials

Channelling radiation: theory vs exp



Comparison of experimentally measured channelling radiation enhancement with theoretical results for 6.7 GeV positrons and electrons in Si(110)

$$\text{Enhancement} = \frac{dE_{\text{Si}(110)}}{dE_{\text{am}}}$$

Figure 4.9: Enhancement factor of the channelling radiation over the radiation in amorphous medium spectrum. The left and right plots are for the positrons and electrons, respectively. Open circles stand for the experimental data from Ref. [8]. Solid curves correspond to the calculations shown in Figure 4.8 and correspond to the zero incident angle, $\psi = 0$. Dashed curves correspond to the calculations with the incident angle lying within $\psi = [-\psi_L, \psi_L]$ with $\psi_L = 62 \mu\text{rad}$. Green dashed line corresponds to results of simulations from the paper [35]. See also explanation in the text.

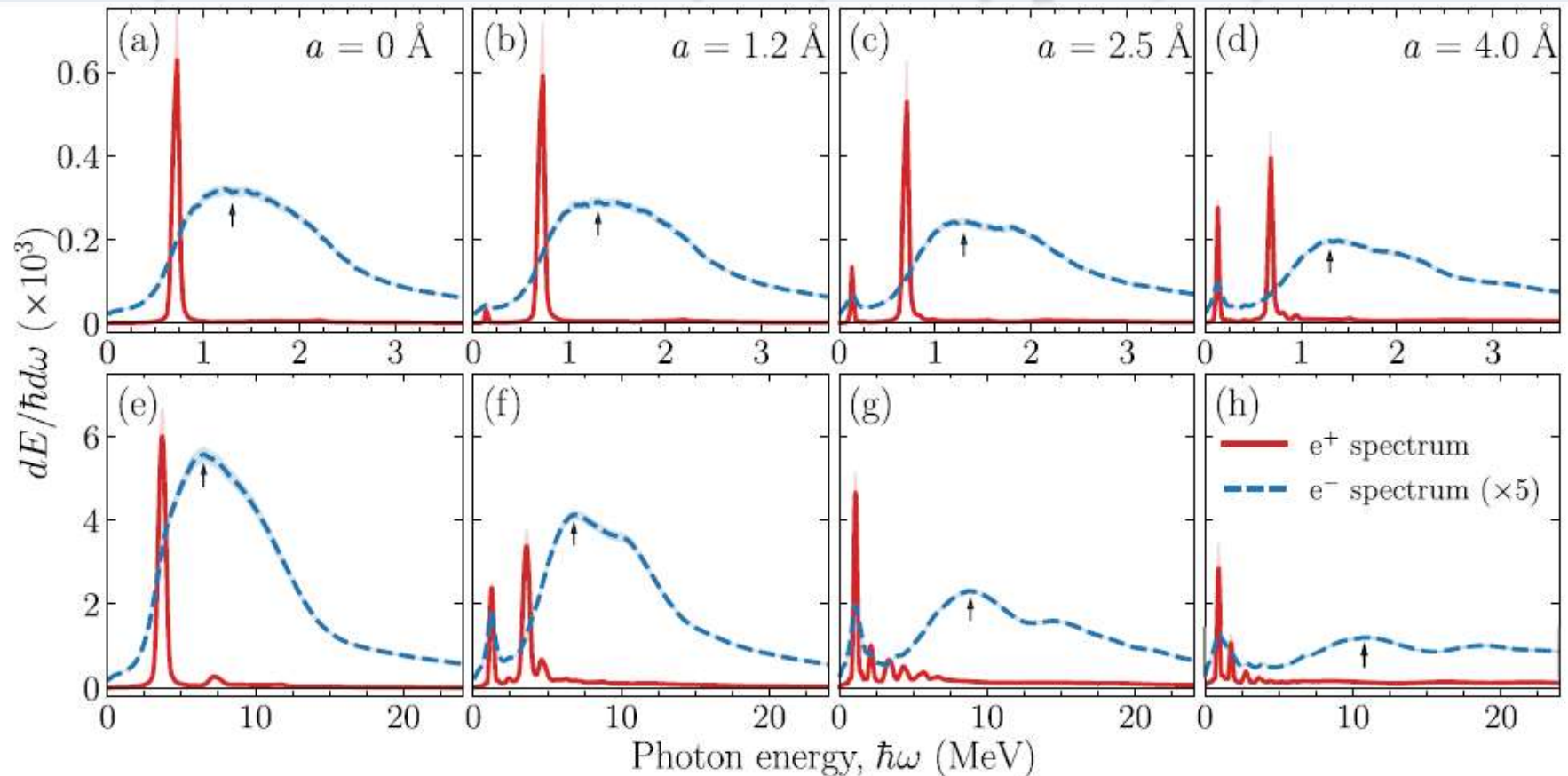
Theory: Sushko, Bezchastnov, Solov'yov, Korol, Greiner, Solov'yov. JCP **252** (2013) 404.

Experiment: J. Bak, J.A. Ellison, E.Uggerhoj et al, Nucl. Phys. B **254** (1985) 491.

Electron and positron emission spectra in 4-periods diamond(110) CU ($\lambda_u=5\text{ }\mu\text{m}$)



MBN
Research Center

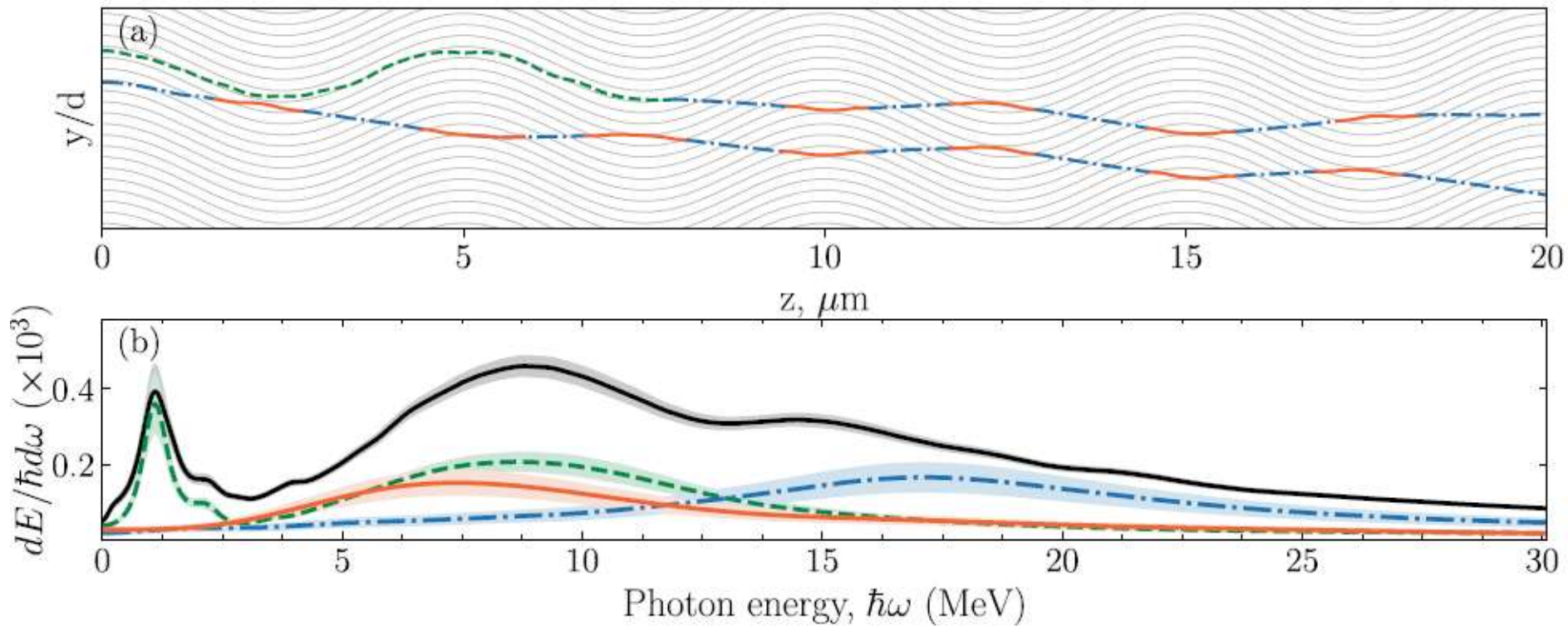


Spectral distribution of radiation for 270 MeV (upper row) and 855 MeV (lower row) **positrons** (red curves) and **electrons** (blue curves). Values of bending amplitudes, a , are as indicated.

Upward arrow show the peaks of the ChR (in straight crystal, $a=0$) and those due to **interplay of ChR** and additional **radiation due to volume reflection**.

A.V. Pavlov, A.V. Korol, V.K. Ivanov, and A.V. Solov'yov, *Eur. Phys. J. D*, vol. 74, 21 (2020)

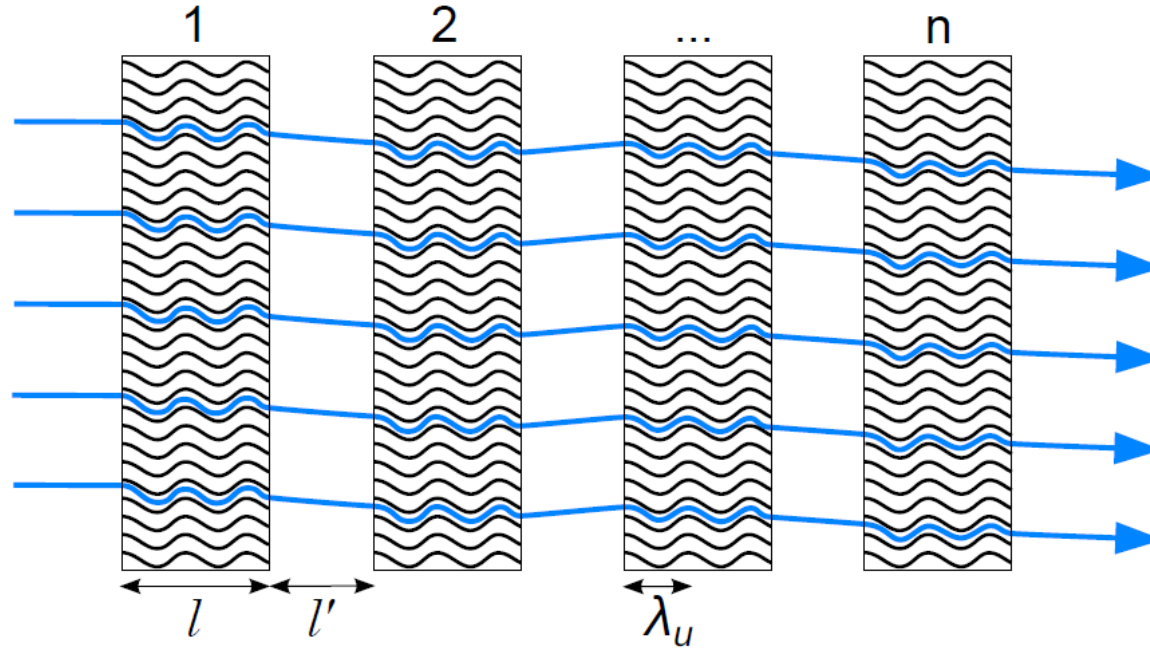
A. Pavlov, V. Ivanov, A. Korol, A. Solov'yov, *J. Phys. B: Atomic, Molecular and Optical Physics*, vol. 52, 11LT01 (2019)



- **Channeling segments** contribute to **CUR and ChR**.
- **Volume-reflection segments** – additional contribution in **the vicinity of the ChR peak**.
- **Over-barrier segments** – produce additional **higher-energy peak**.

A.V. Pavlov, A.V. Korol, V.K. Ivanov, and A.V. Solov'yov, Eur. Phys. J. D, vol. 74, 21 (2020)

Construction of thick bent crystals is a challenge which can be bypassed by introducing a stack of CUs:



- Each layer of stack is the SASP/LALP bent crystal
- The width of each layer \ll the dechanneling length
- The radiation of projectile grows approx. linearly with the number of layers

Sushko, Korol, Solov'yov. *SPB Polytechn. Uni. J: Phys & Math (Elsivier)* **1** (2015) 341

G. Sushko, *Atomistic molecular dynamics approach for channeling of charged particles in oriented crystals*, PhD Thesis, Frankfurt am Main (2015)

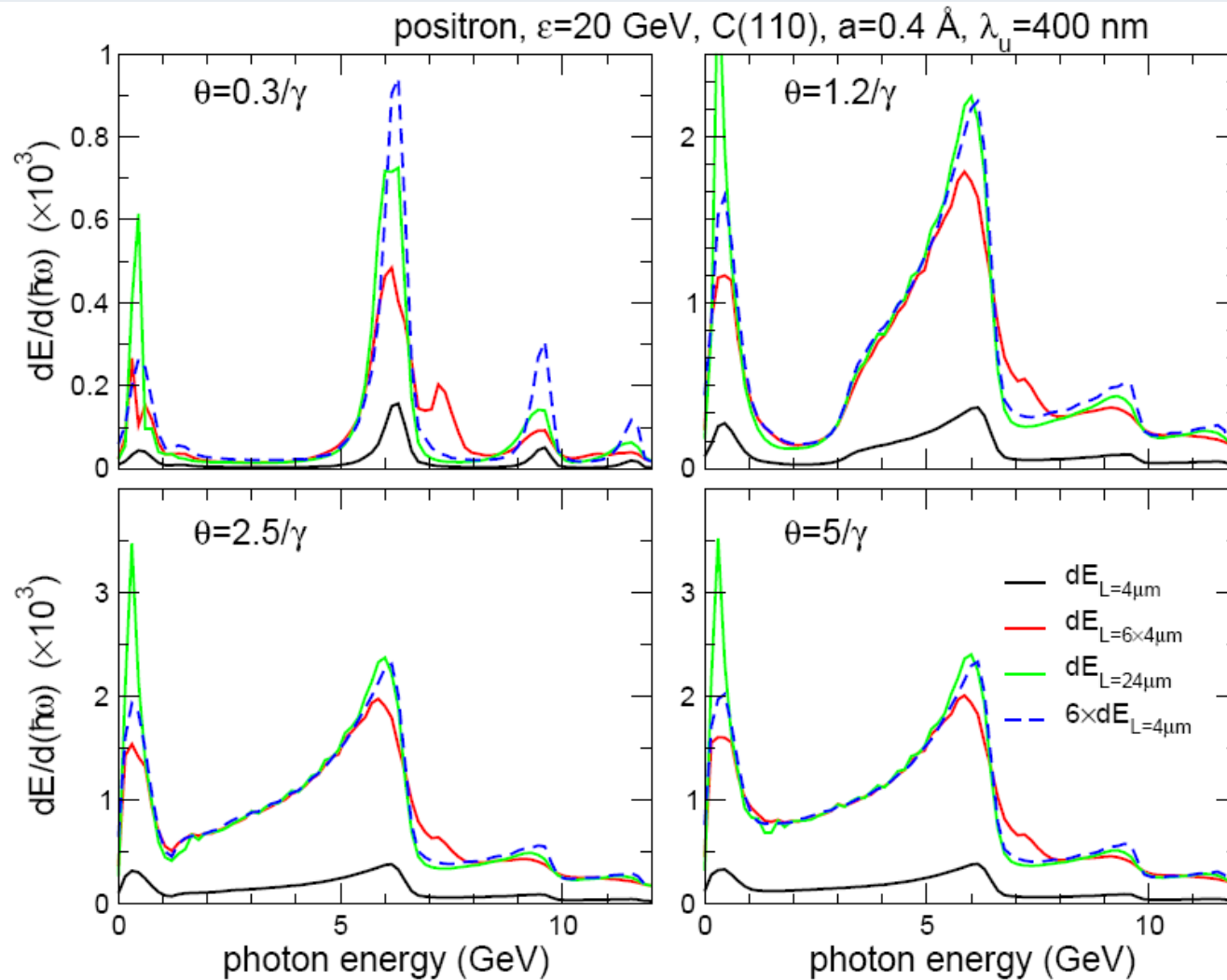


Figure 6. Stack vs $L = 4$ micron.

Brilliance of crystalline undulators

Brilliance of a photon source relates the number of photons of a given energy emitted per unit time interval, unit source area, unit solid angle and per bandwidth (K-J Kim, Nucl. Instrum. Meth. A **246** (1986) 71):

$$B_n = \frac{\Delta N_{\omega_n}}{10^3 (\Delta \omega_n / \omega_n) (2\pi)^2 \varepsilon_x \varepsilon_y} \frac{I}{e}$$

$\omega_n, \Delta \omega_n$ – energy and width of the n th harmonic

$\Delta \omega_n / \omega_n$ – bandwidth (=BW)

ΔN_{ω_n} – number of photons with

$$\omega \in \left[\omega_n - \Delta \omega_n / 2, \omega_n + \Delta \omega_n / 2 \right]$$

I – electric current of the beam

$\varepsilon_{x,y}$ – emittance of the photon source along x, y

$$\varepsilon_{x,y} = \sqrt{\sigma_n^2 + \sigma_{x,y}^2} \sqrt{\phi_n^2 + \phi_{x,y}^2}$$

$$\epsilon_{x,y} = \sqrt{\sigma_n^2 + \sigma_{x,y}^2} \sqrt{\phi_n^2 + \phi_{x,y}^2}$$

Parameters of the *positron* beam

$\sigma_{x,y}$	beam sizes in the x,y directions
$\phi_{x,y}$	angular divergencies of the beam in the x,y directions

Parameters of the *photon* beam

$\phi_n = \sqrt{\Delta\Omega_n/2\pi}$	angular width of the n -th harmonic the 'apparent' source size
$\sigma_n = \lambda_n/4\pi\phi_n$	

$$\Delta N_{\omega_n} = 4\pi\alpha n\zeta \left[J_{\frac{n-1}{2}}(n\zeta) - J_{\frac{n+1}{2}}(n\zeta) \right]^2 N_{\text{eff}} \frac{\Delta\omega_n}{\omega_n}$$

where $\zeta = K^2/(4 + 2K^2)$, $J_\nu(n\zeta)$ is the Bessel function and $K = 2\pi\gamma a/\lambda_u$ is the undulator parameter.

$N_{\text{eff}} = N_{\text{eff}}(N_d, x, \kappa_d)$ is the effective number of undulator periods.

$N_d = L_d/\lambda_u$	Number of periods within dechanneling length L_d
$K_d = L/L_d$	Crystal length / Dechanneling length
$X = L_d/L_a$	Dechanneling length / Attenuation length

$$N_{\text{eff}} = \frac{4N_d}{x\kappa_d} \left[\frac{xe^{-x\kappa_d}}{(1-x)(2-x)} - \frac{e^{-\kappa_d}}{1-x} + \frac{2e^{-(2+x)\kappa_d/2}}{2-x} \right] \sqrt{1 + \kappa_d^2 \frac{(x-1)^2 + 1}{4\pi^2}}$$

- Fix crystal & crystallographic direction;
- Fix parameters of the **positron** beam:
 - » energy ε ,
 - » size $\sigma_{x,y}$ and divergence $\phi_{x,y}$,
 - » beam current I (or, **peak current** I_{\max}).
- Scan over photon energy ω .
- For fixed ω :
 - » Determine $L_{\text{att}}(\omega)$.
 - » Scan over a and λ_u consistent with $C \equiv (2\pi)^2 \frac{\varepsilon}{qU'_{\max}} \frac{a}{\lambda^2} \ll 1$
 - » Determine $L_d = L_d(\varepsilon, C)$
 - » Determine optimal length L_{opt}
 - » **Calculate peak brilliance**

Available positron beams

Table B1. Parameters of positron beams: beam energy, ε , bunch length, L_b , number of particles per bunch, \mathcal{N} , beam size, $\sigma_{x,y}$, beam divergence $\phi_{x,y}$, volume density $n = \mathcal{N}/(\pi\sigma_x\sigma_y L_b)$ of positrons in the bunch, peak current $I_{\max} = e\mathcal{N}c/L_b$ of several positron beams.

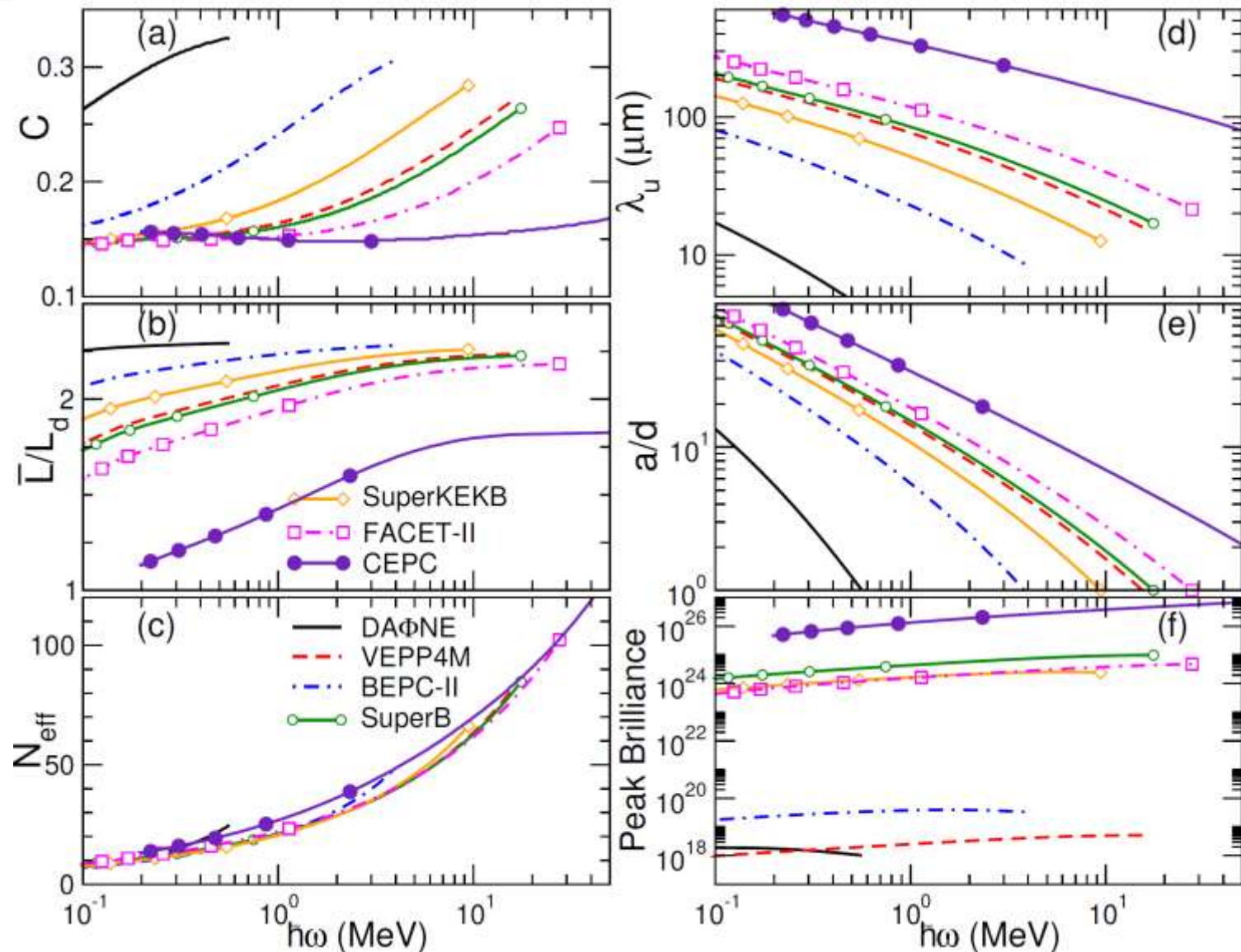
Facility Ref.	VEPP4M [43]	BEPCII [43]	DAΦNE [43]	SuperKEKB [43]	SuperB [45, 46]	FACET-II [44]	CEPC [33]
ε (GeV)	6	1.9-2.3	0.51	4	6.7	10	45.5
\mathcal{N} (units 10^{10})	15	3.8	2.1	9.04	6.5	0.375	8
L_b (cm)	5	1.2	1-2	0.6	0.5	0.00076	0.85
σ_x (μm)	1000	347	260	10	8	10.1	6
σ_y (μm)	30	4.5	4.8	0.048	0.04	7.3	0.04
ϕ_x (mrad)	0.2	0.35	1	0.32	0.250	0.178	0.03
ϕ_y (mrad)	0.67	0.35	0.54	0.18	0.125	0.044	0.04
I_{\max} (A)	144	152	50-100	723	624	12.1×10^3	452
n (10^{13}cm^{-3})	3.2	65	54	1.0×10^6	1.3×10^6	2×10^5	1.25×10^6

[43,45] Particle data group (2018, 2010); [33] CEPC Conceptual Design Report; [44] SLAC-R-1067

Diamond-based optimal CU



MBN
Research Center

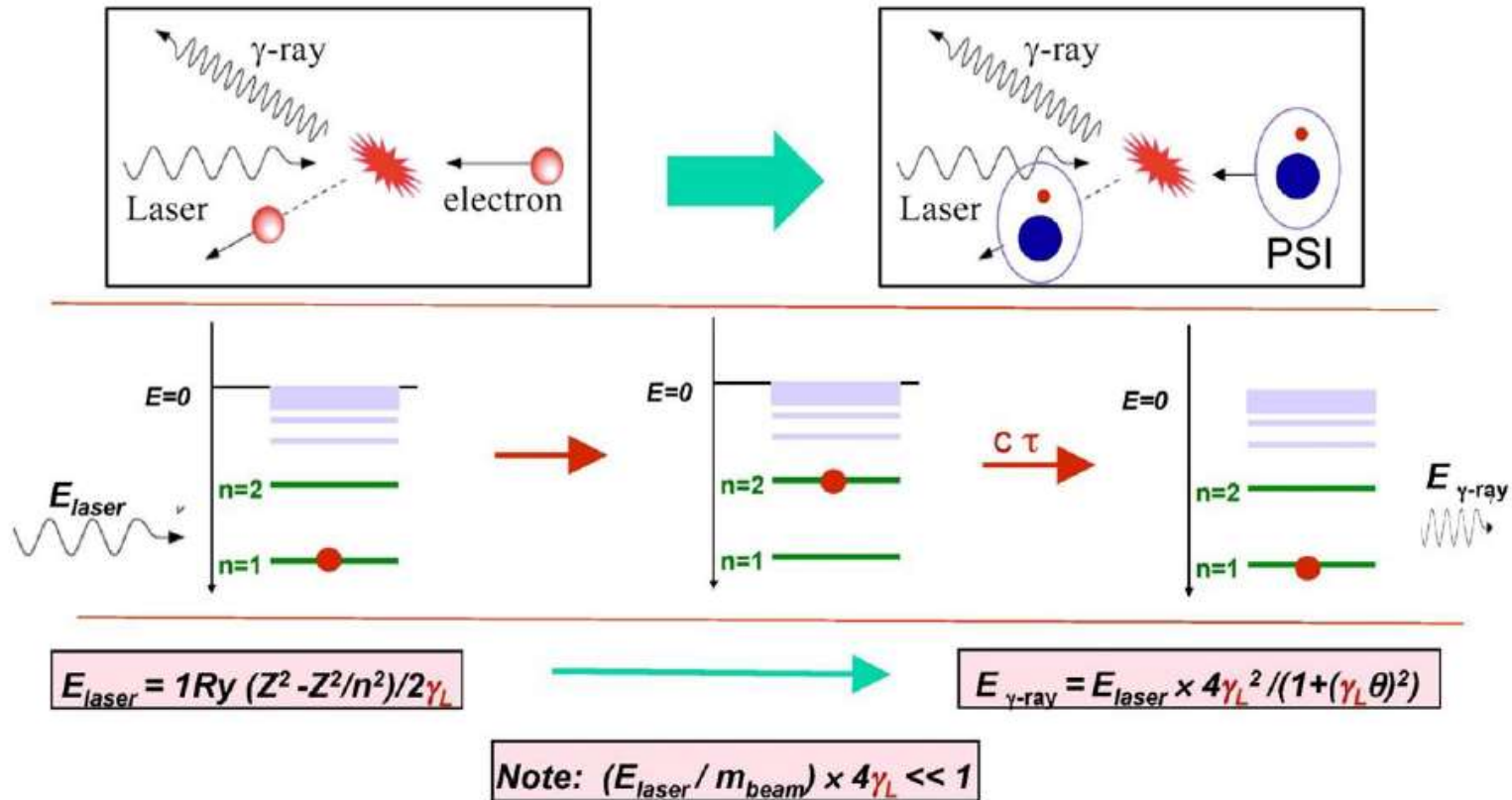


Korol, Solov'yov Arxiv 1910.13359 (2019)

March 16, 2020

MBN Research Center (www.mbnresearch.com)

Laser Compton scattering and CERN photon factory



W. Krasny

FCC based Gamma Factory could provide $>10^{17} e^+/s$

high photon energies,
high cross section

In the process of the resonant absorption of the laser photons by the Partially Stripped Ion (PSI) beam, followed by a spontaneous atomic-transition emissions of secondary photons, the initial laser-photon frequency is boosted by a factor of up to $4\gamma_L^2$, where γ_L is the Lorentz factor of the partially stripped ion beam. Therefore, the light source in the energy range of $1 < E_{\text{photon}} < 400$ MeV must be driven by the high-L, LHC-stored, PSI beams. CERN is a unique place in the world where such a light source could be realized.

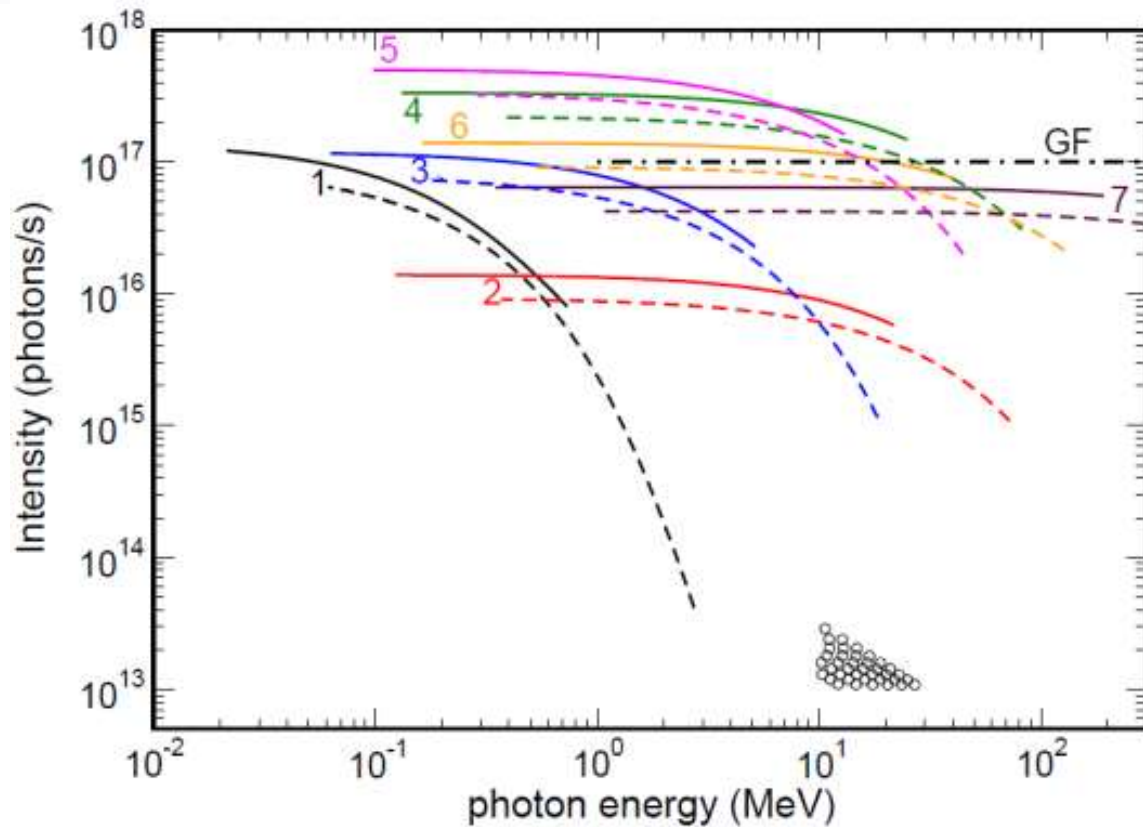
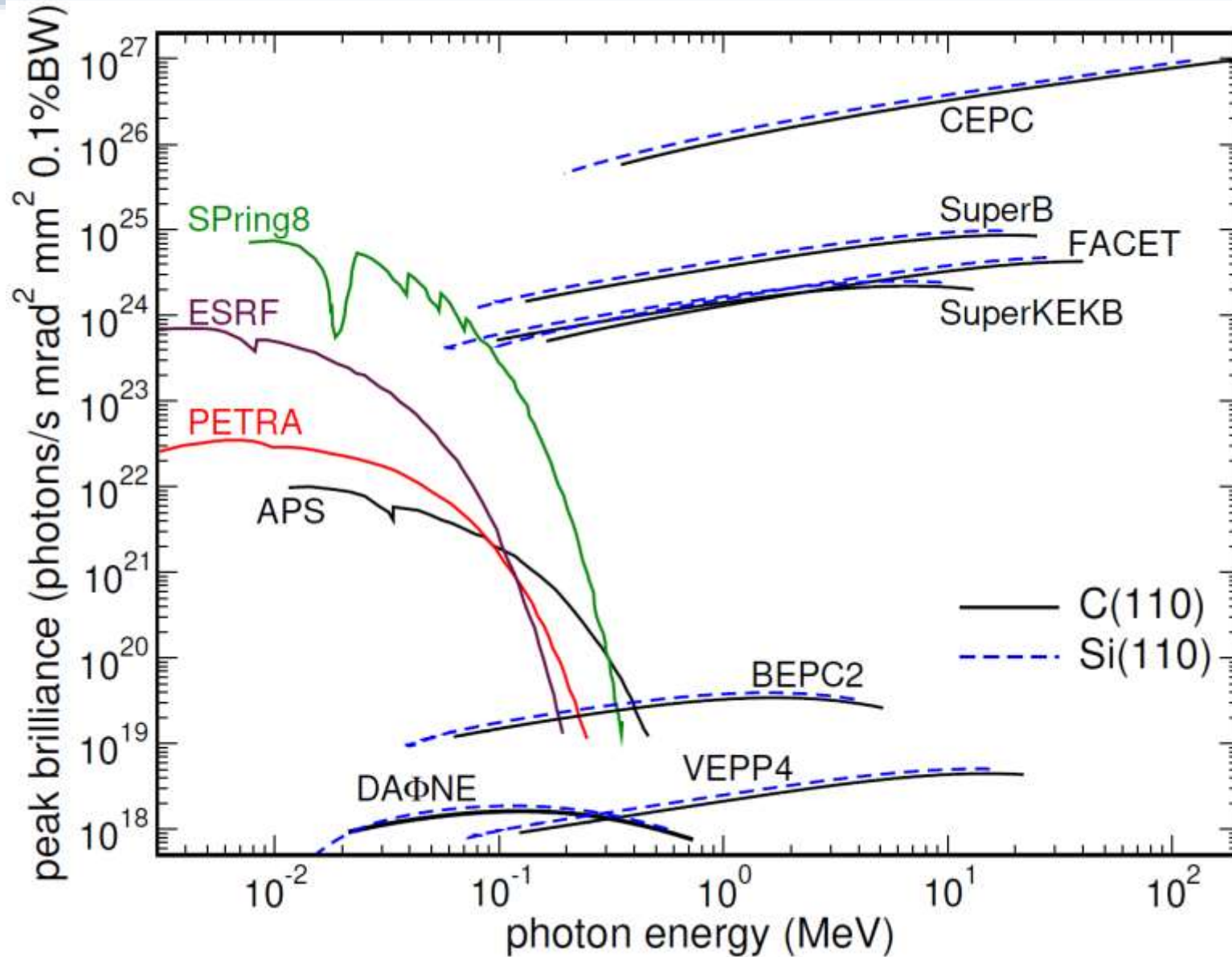


Figure 4. Peak intensity (number of photons per second, $\Delta N_{\omega} I_{\max}/e$) of diamond(110)-based CUs calculated for positron beams at different facilities: 1 - DAΦNE, 2 - VEPP4M, 3 - BEPC-II, 4 - SuperB, 5 - SuperKEK, 6 - FACET-II, 7 - CEPC. Solid and dashed lines correspond to the emission in the first and third harmonics, respectively. Open circles indicate the data on the laser-Compton backscattering [42]. The horizontal dash-dotted line marks the intensity 10^{17} photon/s indicated in the Gamma Factory (GF) proposal for CERN [3].

CU-LS versus synchrotron radiation



MBN
Research Center



Conclusions and outlook

- Atomistic level simulations of particle propagation and photon emission in oriented crystals (linear, bent, PBBs, etc) have a predictive power
- Further experiments with high energy and quality electrons and positrons beams on verification of theoretical predictions are needed
- Further advances in technologies for manufacturing HQ crystals with desired properties (e.g. periodicity, composition, quality, size, etc)
- Design and construction of oriented crystal based light sources with unique properties
- An utmost goal: adopting FEL principles to CU-based Superradiant light sources operating with modulated beams of electrons and positrons
- Growing International Community in the R&D area of oriented crystal based light sources

Concluding remarks

- **MBN Explorer & Studio software** is a powerful instrument of modern theoretical and computational research opening a wide range new possibilities in unravelling structure and dynamics of complex Meso-Bio-Nano (MBN) systems.
- **MBN Explorer & Studio software** enables atomistic level simulations for ultrarelativistic particle propagation and radiation in oriented crystals
- **MBN Explorer & Studio** is being developed by the MBN Research Center, www.mbnresearch.com in Frankfurt. **You are welcome to contact us!**

